

The Next-to-Minimal Supersymmetric Model Close to the R-symmetry Limit and Naturalness in $h \rightarrow aa$ Decays for $m_a < 2m_b$.

Radovan Dermíšek^{1,*} and John F. Gunion^{2,†}

¹*School of Natural Sciences, Institute for Advanced Study, Princeton, NJ 08540*

²*Department of Physics, University of California at Davis, Davis, CA 95616*

(Dated: April 18, 2007)

Abstract

Dominant decay of a SM-like Higgs boson into particles beyond those contained in the minimal supersymmetric standard model has been identified as a natural scenario to avoid fine tuning in electroweak symmetry breaking while satisfying all LEP limits. In the simplest such extension, the next-to-minimal supersymmetric model, the lightest CP-even Higgs boson can decay into two pseudoscalars. In the scenario with least fine tuning the lightest CP-even Higgs boson has mass of order 100 GeV. In order to escape LEP limits it must decay to a pair of the lightest CP-odd Higgs bosons with $\text{Br}(h \rightarrow aa) > .7$ and $m_a < 2m_b$ (so that $a \rightarrow \tau^+\tau^-$ or light quarks and gluons). The mass of the lightest CP-odd Higgs boson is controlled by the soft-trilinear couplings, $A_\lambda(m_Z)$ and $A_\kappa(m_Z)$. We identify the region of parameter space where this situation occurs and discuss how natural this scenario is. It turns out that in order to achieve $m_a < 2m_b$ with $A_\lambda(m_Z)$, $A_\kappa(m_Z)$ of order the typical radiative corrections, the required tuning of trilinear couplings need not be larger than 5-10 %. Further, the necessity for this tuning can be eliminated in specific SUSY breaking scenarios. Quite interestingly, $\text{Br}(h \rightarrow aa)$ is typically above 70 % in this region of parameter space and thus an appropriately large value requires no additional tuning.

*dermisek@ias.edu

†gunion@physics.ucdavis.edu

I. INTRODUCTION

The Minimal Supersymmetric Standard Model (MSSM) is a widely studied possibility for physics beyond the standard model (SM). Its content in the matter and gauge sectors is fixed by all known particles and assumed superpartners. However, the choice of a two-doublet Higgs sector is made purely on the basis of minimality arguments. It is exactly the Higgs sector, namely the non-observation of the Higgs boson, that casts a shadow on the whole MSSM. It is becoming obvious that if the MSSM is the correct description of nature then the supersymmetric (SUSY) spectrum has to be quite unusual: heavy enough that sparticles escape direct detection, but not so heavy that electroweak symmetry breaking becomes unnatural. And, if the sparticles are not particularly heavy, the MSSM parameters must be special enough that the Higgs boson mass is pushed (through radiative corrections) above the experimental bound.¹ Another possibility, which does not require any special assumptions about the SUSY spectrum and parameters, is to abandon the minimal Higgs sector, for which there was never any deep reason anyway and which gives rise to the famous μ -problem. In this case, the expectations for Higgs phenomenology are modified and the tension from not having observed the Higgs boson at LEP can be eliminated [3].

A particularly appealing extension of the SM or MSSM is the introduction of a completely new sector of particles which are singlets under the SM gauge symmetry. As such, this extra (E) sector would not spoil any of the virtues of the MSSM, including the possibility of gauge coupling unification and matter particles fitting into complete GUT multiplets. In addition, E-sector particles would have easily escaped direct detection. Of course, if this E-sector is completely decoupled from the SM then it plays no role in particle physics phenomenology at accelerators. However, it is possible that this sector couples to the MSSM through the Higgs fields. For example, the superpotential can contain a term in which the two Higgs doublets are combined in a SM-singlet form. Without additional Higgs fields, the coefficient of this form must have dimensions of mass, and the resulting superpotential component is the so-called μ -term. In contrast, the E-sector can couple to this SM-singlet form in many

¹ Scenarios that lead to such a special SUSY spectrum were recently found, see for example mixed anomaly-modulus mediation [1] or gauge mediation with gauge messengers [2]. Both scenarios generate large mixing in the stop sector which maximizes the Higgs mass, allowing all experimental limits to be satisfied with a fairly light SUSY spectrum.

ways, including at the renormalizable (dimensionless coupling) level. Such couplings would have a negligible effect on the phenomenology involving SM matter fields, whereas they can dramatically alter Higgs physics. For example, they would allow the lightest CP-even Higgs boson h to decay into two of these E-fields if the E-fields are light enough. In that case, the usual Higgs decay mode, $h \rightarrow b\bar{b}$, might no longer be dominant and, since the $hb\bar{b}$ coupling is small, $\text{Br}(h \rightarrow b\bar{b})$ can be suppressed by a large factor. The strategy for Higgs discovery would then depend on the way the E-fields appearing in the decays of the h themselves decay. They might decay predominantly into other stable E-fields, in which case the MSSM-like h decays mainly invisibly. If such decays are kinematically impossible or suppressed, then, given that couplings between the MSSM and E-sector Higgs fields are generically present and imply that the mass eigenstates are mixed, the mostly E-field light Higgses will decay into $b\bar{b}$, $\tau^+\tau^-$ or other quarks or leptons depending on the model. Although E-particles would have small direct production cross sections and it would be difficult to detect them directly, their presence would be manifest through the dominant Higgs decay modes being $h \rightarrow 4f$, where $4f$ symbolically means four SM fields, *e.g.* $b\bar{b}b\bar{b}$, $b\bar{b}\tau^+\tau^-$, $\tau^+\tau^-\tau^+\tau^-$, 4γ and so on ². This would imply a very complicated Higgs phenomenology. Nevertheless, such a scenario is a simple consequence of having an extra sector which couples to the SM or MSSM through mixing of the Higgs sectors with one of the extra Higgs mass eigenstates being light enough that the SM-like Higgs can decay into a pair them.

The situation described in the previous paragraph already occurs in the simplest extension of the MSSM, the next-to-minimal supersymmetric model (NMSSM) which adds only one singlet chiral superfield, \widehat{S} . The very attractive nature of the NMSSM extension of the MSSM on general grounds has been discussed for many years [4]; in particular, it avoids the need for the μ parameter of the MSSM superpotential term $\mu\widehat{H}_u\widehat{H}_d$. The NMSSM particle content differs from the MSSM by the addition of one CP-even and one CP-odd state in the neutral Higgs sector (assuming CP conservation), and one additional neutralino. We will follow the conventions of [5]. Apart from the usual quark and lepton Yukawa couplings, the scale invariant superpotential is

$$\lambda \widehat{S}\widehat{H}_u\widehat{H}_d + \frac{\kappa}{3} \widehat{S}^3 \quad (1)$$

² The situation can be even more complicated if the E-field decays into other E-fields before the latter finally decay to SM fields. In such a case, the SM-like Higgs would effectively decay into $8f$. Even more complicated variations can also be constructed.

depending on two dimensionless couplings λ, κ beyond the MSSM. [Hatted (unhatted) capital letters denote superfields (scalar superfield components).] An effective μ term arises from the first term of Eq. (1) when the scalar component of \widehat{S} acquires a vacuum expectation value, $s \equiv \langle \widehat{S} \rangle$, yielding

$$\mu_{\text{eff}} = \lambda s. \quad (2)$$

The trilinear soft terms associated with the superpotential terms in Eq. (1) are

$$\lambda A_\lambda S H_u H_d + \frac{\kappa}{3} A_\kappa S^3. \quad (3)$$

The final input parameter is

$$\tan \beta = h_u / h_d, \quad (4)$$

where $h_u \equiv \langle H_u \rangle$, $h_d \equiv \langle H_d \rangle$. The vevs h_u , h_d and s , along with m_Z , can be viewed as determining the three SUSY breaking masses squared for H_u , H_d and S (denoted $m_{H_u}^2$, $m_{H_d}^2$ and m_S^2) through the three minimization equations of the scalar potential. Thus, as compared to the three independent parameters needed in the MSSM context (often chosen as μ , $\tan \beta$ and M_A), the Higgs sector of the NMSSM is described by the six parameters

$$\lambda, \kappa, A_\lambda, A_\kappa, \tan \beta, \mu_{\text{eff}}. \quad (5)$$

(We employ a convention in which all parameters are evaluated at scale m_Z unless otherwise stated.) We will choose sign conventions for the fields such that λ and $\tan \beta$ are positive, while κ , A_λ , A_κ and μ_{eff} should be allowed to have either sign. In addition, values must be input for the gaugino masses ($M_{1,2,3}$) and for the soft terms related to the (third generation) squarks and sleptons ($m_Q^2, m_U^2, m_D^2, m_L^2, m_E^2, A_t, A_b$ and A_τ) that contribute to the radiative corrections in the Higgs sector and to the Higgs decay widths. For moderate $\tan \beta$, the soft parameters which play the most prominent role are m_Q^2, m_U^2, m_D^2 and A_t .

Of all the possible new phenomena, the additional Higgses in the NMSSM can lead to, perhaps the most intriguing one is the possibility of the lightest CP-even Higgs decaying into a pair of the two lightest CP-odd Higgses, $h_1 \rightarrow a_1 a_1$, where the latter are mostly singlets [3, 6, 7, 8, 9]. Not only would $h_1 \rightarrow a_1 a_1$ decays complicate Higgs searches, but also it is found that precisely this scenario can essentially eliminate the fine tuning of EWSB in the NMSSM for $m_{h_1} \sim 100$ GeV [3, 7, 8]. If $\text{Br}(h_1 \rightarrow a_1 a_1) > 0.7$ and $m_{a_1} < 2m_b$, the usual (LEP) limit on the Higgs boson mass does not apply and the SUSY spectrum can be arbitrarily light, perhaps just above the experimental bounds, *i.e.* certainly light enough for natural EWSB [3, 7, 8].

In this paper, we identify the region of parameter space where this situation occurs and discuss how natural this scenario is. The mass of the lightest CP-odd Higgs boson is controlled by the soft-trilinear couplings A_λ and A_κ and vanishes in the R-symmetry limit, $A_\lambda, A_\kappa \rightarrow 0$. However, both A_λ and A_κ receive radiative corrections from gaugino masses and so arbitrarily small values of trilinear couplings would require cancellation between the bare values and the radiative corrections. It turns out that in order to achieve $m_{a_1} < 2m_b$ with A_λ, A_κ of order the typical radiative corrections, a tuning of trilinear couplings at the level of 5% – 10% might be required, but that even less fine-tuning is possible in the context of various types of models. Quite interestingly, $\text{Br}(h_1 \rightarrow a_1 a_1) > 70\%$ is automatic in this region of parameter space, implying no need for additional tuning in order to achieve $\text{Br}(h_1 \rightarrow b\bar{b})$ small enough to escape LEP limits³.

It is important to note that to a large extent the tuning in A_λ and A_κ required for $\text{Br}(h_1 \rightarrow a_1 a_1) > 0.7$ and $m_{a_1} < 2m_b$ can be separated from fine-tuning/naturalness for proper EWSB. The value of m_Z , as obtained from the renormalization group (RG) equations after evolving from the GUT-scale, M_U , down to m_Z , is primarily sensitive to $M_3(M_U)$, $m_{H_u}^2(M_U)$, $m_{H_d}^2(M_U)$, $m_S^2(M_U)$, $m_Q^2(M_U)$, $m_U^2(M_U)$, $m_D^2(M_U)$, and $A_t(M_U)$ (and $A_b(M_U)$ if $\tan\beta$ is large). In some cases, $M_2(M_U)$ can contribute significantly to the standard measure of EWSB fine-tuning with respect to the GUT-scale parameters. In contrast, $M_1(M_U)$, $A_\lambda(M_U)$, and $A_\kappa(M_U)$ have to take very large values in order to contribute significantly to fine-tuning. The scenarios that have small fine-tuning that we focus on are ones in which these parameters are small enough that they do not affect the measure of the fine-tuning associated with EWSB. In a companion paper [8], we discuss EWSB fine-tuning in detail, expanding upon the earlier discussions in Refs. [3, 7].

Recently various scenarios, similar in spirit, which improve on the naturalness of EWSB by modifying Higgs decays or which, in general, suggest the possibility of an extra sector near the EW scale have been discussed; see *e.g.* [11, 12, 13, 14]. Phenomenological consequences

³ Some aspects of EWSB and the possibility of having a light CP-odd Higgs boson in the NMSSM in the R-symmetry limit were also recently discussed in Ref. [10]. Results and conclusions presented in Ref. [10] are based on studying a region of parameter space very near the R-symmetry limit with soft-trilinear couplings much below the typical size of radiative corrections. The conclusions of this reference do not necessarily apply to the scenario discussed above that assumes soft-trilinear couplings A_λ and A_κ of order the typical radiative corrections (they could, however, originate from an exact symmetry limit at some high scale). We refer to our scenario as *NMSSM close to the R-symmetry limit*.

and possible collider signatures for the NMSSM and, more specifically, for some of these scenarios have also been discussed in Refs. [15, 16, 17, 18].

The paper is organized as follows. In the next section, we discuss the NMSSM close to the R-symmetry limit. Numerical results are presented in Sec. III and we conclude in Sec. IV.

II. NMSSM CLOSE TO THE R-SYMMETRY LIMIT

In the NMSSM, one of the CP-odd Higgses is massless in the Peccei-Quinn symmetry limit, $\kappa \rightarrow 0$, or in the R-symmetry limit, $A_\kappa, A_\lambda \rightarrow 0$ [9]. We focus here on the second case because it was identified as the easiest way to achieve EWSB without large fine tuning in soft SUSY breaking terms [3]. This scenario requires that the lightest CP-even Higgs boson, h_1 , decays to a pair of the lightest CP-odd Higgs bosons with $\text{Br}(h_1 \rightarrow a_1 a_1)$ large enough that the $h_1 \rightarrow b\bar{b}$ signal is highly reduced (compared to the SM signal). Furthermore, it was found that this scenario with reduced $\text{Br}(h_1 \rightarrow b\bar{b})$ is consistent with the observed excess of events at $m_h \simeq 100$ GeV in Zh production at LEP [7].

The masslessness of a_1 in the limit $A_\kappa, A_\lambda \rightarrow 0$ can be understood as a consequence of a global $U(1)_R$ symmetry of the superpotential under which the charge of S is half of the charge of $H_u H_d$. In the limit $A_\kappa, A_\lambda \rightarrow 0$ it is also a symmetry of the scalar potential. This symmetry is spontaneously broken by the vevs of H_u , H_d and S , resulting in a Nambu-Goldstone boson in the spectrum. Soft trilinear couplings explicitly break $U(1)_R$ and thus lift the mass of the a_1 . For small trilinear couplings, the mass of the lightest CP-odd Higgs boson is approximately given as:

$$m_{a_1}^2 \simeq 3s \left(\frac{3\lambda A_\lambda \cos^2 \theta_A}{2 \sin 2\beta} - \kappa A_\kappa \sin^2 \theta_A \right), \quad (6)$$

where $\cos \theta_A$ measures the doublet component of the lightest CP-odd Higgs mass eigenstate,

$$a_1 = \cos \theta_A A_{MSSM} + \sin \theta_A A_S. \quad (7)$$

In the limit of large $\tan \beta$ or $|s| \gg v$, $\cos \theta_A$ can be approximated by

$$\cos \theta_A \simeq \frac{v \sin 2\beta}{s}. \quad (8)$$

In this limit, the a_1 mass eigenstate is mostly singlet and

$$m_{a_1}^2 \sim 3s \left(\frac{3\lambda A_\lambda v^2 \sin 2\beta}{2s^2} - \kappa A_\kappa \right). \quad (9)$$

Naively, an arbitrarily small mass for the a_1 is achievable provided small values of A_κ and A_λ are generated by a SUSY breaking scenario. Indeed, there are SUSY breaking scenarios, *e.g.* gauge mediation or gaugino mediation, which have zero soft trilinear couplings in the leading order. However, even if zero values of A_κ and A_λ are generated at the SUSY breaking scale, the corresponding electroweak (EW) scale values will be shifted due to radiative corrections from gaugino masses. The typical EW scale values can be estimated from the one-loop renormalization group equations for A_λ and A_κ ,

$$\frac{dA_\lambda}{dt} = \frac{1}{16\pi^2} \left[6A_t\lambda_t^2 + 8\lambda^2 A_\lambda + 4\kappa^2 A_\kappa + 6g_2^2 M_2 + \left(\frac{6}{5}\right) g_1^2 M_1 \right], \quad (10)$$

$$\frac{dA_\kappa}{dt} = \frac{12}{16\pi^2} (\lambda^2 A_\lambda + \kappa^2 A_\kappa), \quad (11)$$

where $t = \log(Q/m_Z)$, A_t is the top soft trilinear coupling and M_2 and M_1 are the masses of the SU(2) and U(1) gauginos, and we have neglected terms proportional to A_b and A_τ . Starting with $A_\lambda = 0$ at the GUT scale, we find that $A_\lambda(m_Z) \sim M_2$ because the $\log(M_U/m_Z)$ coming from the integration approximately cancels the $(6g_2^2)/(16\pi^2)$ loop factor. On the other hand, A_κ receives contributions from gaugino masses only at the two-loop level implying that $A_\kappa(m_Z)$ is expected to be much smaller than $A_\lambda(m_Z)$. Assuming gaugino masses of order 100 GeV, we should naturally expect $A_\lambda(m_Z) \simeq 100$ GeV and $A_\kappa(m_Z) \sim \text{few GeV}$. Much smaller values would require cancellations between the values of A_λ , A_κ coming from a particular SUSY breaking scenario and the contributions from the radiative corrections.

For sizable $A_\lambda(m_Z)$, Eq. (9) is no longer a good approximation for the mass of the lightest CP-odd Higgs. In order to understand the numerical results presented later, we have developed a more accurate formula. The 2×2 mass matrix squared for the CP-odd Higgs bosons, in the basis (A_{MSSM}, A_S) , has the following matrix elements [5]:

$$M_{11}^2 = \frac{2\lambda s}{\sin 2\beta} (A_\lambda + \kappa s), \quad (12)$$

$$M_{12}^2 = \lambda v (A_\lambda - 2\kappa s), \quad (13)$$

$$M_{22}^2 = 2\lambda\kappa v^2 \sin 2\beta + \lambda A_\lambda \frac{v^2 \sin 2\beta}{2s} - 3\kappa A_\kappa s. \quad (14)$$

The eigenstate masses are

$$m_{a_1}^2 = \frac{1}{2} \left[M_{11}^2 + M_{22}^2 \mp \sqrt{(M_{11}^2 - M_{22}^2)^2 + 4(M_{12}^2)^2} \right]. \quad (15)$$

The mixing angle for the diagonalization process is obtained from

$$\sin 2\theta_A = -\frac{2M_{12}^2}{\sqrt{(M_{11}^2 - M_{22}^2)^2 + 4(M_{12}^2)^2}} \quad (16)$$

$$\cos 2\theta_A = -\frac{M_{11}^2 - M_{22}^2}{\sqrt{(M_{11}^2 - M_{22}^2)^2 + 4(M_{12}^2)^2}}, \quad (17)$$

where we are using the convention defined in Eq. (7). Obviously, the value of θ_A is only determined mod(π). In our numerical work, we employ the program NMHDECAY[5] which adopts the convention $0 \leq \theta_A \leq \pi$. If M_{11}^2 is much larger in magnitude than the other entries, then it must be positive and the mass squared of the lightest CP-odd Higgs boson is then given by

$$m_{a_1}^2 \simeq \frac{M_{11}^2 M_{22}^2 - (M_{12}^2)^2}{M_{11}^2 + M_{22}^2}. \quad (18)$$

For typical values of trilinear couplings, $|A_\kappa| \ll |A_\lambda| \sim v \ll |s|$, and $\tan \beta \gtrsim few$ we find:

$$m_{a_1}^2 \simeq 3s \left(\frac{3\kappa\lambda^2 A_\lambda v^2}{\frac{2\lambda s}{\sin 2\beta}(A_\lambda + \kappa s) - 3\kappa A_\kappa s} - \kappa A_\kappa \right), \quad (19)$$

which reduces to Eq. (9) if we neglect A_λ and A_κ compared to s . Similarly, the mixing angle is determined by

$$\cos 2\theta_A = 2 \cos^2 \theta_A - 1 \simeq \frac{2(M_{12}^2)^2}{(M_{11}^2 - M_{22}^2)^2} - 1, \quad (20)$$

$$\sin 2\theta_A = 2 \sin \theta_A \cos \theta_A \simeq -\frac{2M_{12}^2}{M_{11}^2 - M_{22}^2}, \quad (21)$$

from which we obtain (using the conventions defined earlier) $\sin \theta_A \sim 1$ and the doublet component of a_1 is given by

$$\cos \theta_A \simeq -\frac{M_{12}^2}{M_{11}^2 - M_{22}^2} \simeq -\frac{\lambda v(A_\lambda - 2\kappa s) \sin 2\beta}{2\lambda s(A_\lambda + \kappa s) + 3\kappa A_\kappa s \sin 2\beta}. \quad (22)$$

This reduces to Eq. (8) for very small A_λ and A_κ .

Both Eq. (9) and Eq. (19) indicate that sizable A_λ could give a large contribution to the mass of the lightest CP-odd Higgs. However this term is highly suppressed if the lightest CP-odd Higgs is mostly singlet. In this case, both terms in Eq. (9) or Eq. (19) are comparable and then it depends on their relative sign as to whether they contribute constructively or destructively. One measure of the tuning in $A_\lambda(m_Z)$ and $A_\kappa(m_Z)$ necessary to achieve $m_{a_1} < 2m_b$ is

$$F_{MAX} = \max \{|F_{A_\lambda}|, |F_{A_\kappa}|\}, \quad (23)$$

where

$$F_{A_\lambda} \equiv \frac{A_\lambda(m_Z)}{m_{a_1}^2} \frac{dm_{a_1}^2}{dA_\lambda(m_Z)}, \quad F_{A_\kappa} \equiv \frac{A_\kappa(m_Z)}{m_{a_1}^2} \frac{dm_{a_1}^2}{dA_\kappa(m_Z)} \quad (24)$$

are evaluated for given choices of $A_\lambda(m_Z)$ and $A_\kappa(m_Z)$ that yield a given m_{a_1} . This definition, which reflects the fact that m_{a_1} is determined by these parameters for fixed $\lambda, \kappa, \mu_{\text{eff}}, \tan \beta$, will prove useful below for discussing the sensitivity of m_{a_1} to GUT-scale parameters. We argue below that F_{MAX} is typically an upper bound on the magnitude of fine tuning with respect to GUT scale parameters. Thus, F_{MAX} provides a useful first measure for determining a “preferred” region of parameter space where a small mass for the lightest CP-odd Higgs boson is achieved with the least tension. However, we will also find that in large classes of models F_{MAX} greatly over-estimates the fine-tuning.

The fine-tuning measure for $m_{a_1}^2$ relative to GUT scale parameters that is completely analogous to that employed for EWSB is

$$F_{m_{a_1}} \equiv \max_p f_p, \quad \text{with} \quad f_p \equiv \frac{d \log m_{a_1}^2}{d \log p}, \quad (25)$$

where p is any GUT-scale parameter,

$$p = M_i \ (i = 1, 2, 3), \ m_{H_u}^2, \ m_{H_d}^2, \ m_S^2, \ A_t, \ A_\kappa, \ A_\lambda, \ m_Q^2, \ m_U^2, \ m_D^2 \quad (26)$$

(to name the most important GUT-scale parameters). However, for our purposes we can simplify this general computation because we are only interested in $m_{a_1}^2$ fine tuning for cases in which the EWSB fine tuning is already known to be small, that is cases in which

$$m_Z^2 = 2 \left[-\lambda^2(m_Z) s^2(m_Z) + \frac{m_{H_d}^2(m_Z) - \tan^2 \beta(m_Z) m_{H_u}^2(m_Z)}{\tan^2 \beta(m_Z) - 1} \right] \quad (27)$$

is insensitive to the parameters p . Small fine tuning for m_Z^2 means that $v(m_Z)$ (which sets m_Z), $s(m_Z)$, $\tan \beta(m_Z)$, $m_{H_u}^2(m_Z)$ and $m_{H_d}^2(m_Z)$ are not fine-tuned with respect to the various p listed above. The only additional parameters upon which $m_{a_1}^2$ depends that could still be sensitive to the GUT-scale parameters p when m_Z is not are $A_\lambda(m_Z)$ and $A_\kappa(m_Z)$. For any of the p , we can then approximate

$$f_p \sim \frac{p}{A_\lambda(m_Z)} F_{A_\lambda} \frac{dA_\lambda(m_Z)}{dp} + \frac{p}{A_\kappa(m_Z)} F_{A_\kappa} \frac{dA_\kappa(m_Z)}{dp}. \quad (28)$$

To understand the implications of this formula, we need to solve the RG equations and express $A_\lambda(m_Z)$ and $A_\kappa(m_Z)$ in terms of the GUT-scale values of all the soft-SUSY-breaking parameters. (Of course, we are taking the GUT scale as an example; a similar exercise can be done for any scale.) The solution depends on λ, κ and $\tan \beta$; we give only a representative

example. For $\lambda = 0.2$, $\kappa = \pm 0.2$ and $\tan \beta = 10$ we find:

$$A_\lambda(m_Z) = -0.03A_\kappa + 0.93A_\lambda - 0.35A_t - 0.03M_1 - 0.37M_2 + 0.66M_3, \quad (29)$$

$$A_\kappa(m_Z) = 0.90A_\kappa - 0.11A_\lambda + 0.02A_t + 0.003M_1 + 0.025M_2 - 0.017M_3, \quad (30)$$

where the parameters on the right-hand side of these equations are the GUT-scale values.

Before discussing the fine-tuning implications of Eqs. (29) and (30), it is useful to understand a few of their features. First, we note that while the coefficients in the $A_\lambda(m_Z)$ expansion do not change much when changing λ and κ , the coefficients in the $A_\kappa(m_Z)$ expansion are quite sensitive to changes of the λ, κ Yukawa couplings. The reason is that gaugino masses enter A_κ through the A_λ term in the RG equation, see Eqs. (10)–(11), the strength of which is controlled by λ . The opposite sign of the coefficient in front of M_3 in the expansion of A_λ as compared to the coefficients in front of M_1 and M_2 is due to the fact that M_3 enters only through A_t in the RG evolution, while both M_1 and M_2 enter directly. Similarly, the opposite sign in front of the gaugino masses in the A_λ expansion as compared to the A_κ expansion is due to the fact that gaugino masses enter A_κ through A_λ in the evolution. The above expansions provide several ways to achieve $A_\kappa \ll A_\lambda \sim m_Z$. The easiest way is to assume that a SUSY breaking scenario generates negligible trilinear couplings at the GUT scale.

We now return to a consideration of the fine-tuning implications of Eqs. (29) and (30). If there is a p_λ that dominates $A_\lambda(m_Z)$ and a p_κ that dominates $A_\kappa(m_Z)$, and these are different, then

$$\frac{p_\lambda}{A_\lambda(m_Z)} \frac{dA_\lambda(m_Z)}{dp_\lambda} \sim \mathcal{O}(1), \quad \text{and} \quad \frac{p_\kappa}{A_\kappa(m_Z)} \frac{dA_\kappa(m_Z)}{dp_\kappa} \sim \mathcal{O}(1), \quad (31)$$

and roughly $F_{m_{a_1}} \sim F_{MAX}$. If the same p dominates both $A_\lambda(m_Z)$ and $A_\kappa(m_Z)$ then $F_{m_{a_1}} \sim f_p \sim F_{A_\lambda} + F_{A_\kappa}$. This result also holds if the GUT-scale parameters are correlated. For example, consider the case of universal gaugino masses and zero trilinear couplings at the GUT scale, for which $A_\lambda(m_Z) = 0.26M_{1/2}$ and $A_\kappa(m_Z) = 0.01M_{1/2}$. Then,

$$\frac{M_{1/2}}{A_\lambda(m_Z)} \frac{dA_\lambda(m_Z)}{dM_{1/2}} = \frac{M_{1/2}}{A_\kappa(m_Z)} \frac{dA_\kappa(m_Z)}{dM_{1/2}} = 1 \quad (32)$$

and it is quite precisely the case that

$$F_{m_{a_1}} = f_{M_{1/2}} \sim F_{A_\lambda} + F_{A_\kappa} \quad (33)$$

As we shall see in the numerical section of this paper, F_{A_λ} and F_{A_κ} are typically opposite in sign and of similar magnitude. This can already be seen from the approximate formula of Eq. (9) where the linearity of $m_{a_1}^2$ in $A_\lambda(m_Z)$ and $A_\kappa(m_Z)$ would give (neglecting the mild dependence of $s(m_Z), \dots$ on $M_{1/2}$ for the points of interest)

$$F_{A_\lambda} + F_{A_\kappa} \sim 1, \quad (34)$$

and fine tuning with respect to $M_{1/2}$ would be small. The more precise (but still approximate) result of Eq. (19) gives somewhat larger results for $F_{A_\lambda} + F_{A_\kappa}$ for some parameter choices, but a subset of choices still gives $F_{A_\lambda} + F_{A_\kappa} \sim \mathcal{O}(1)$. Later, we will present numerical results for F_{A_λ} and F_{A_κ} that confirm that they largely cancel against one another for a significant fraction of parameter choices. The result of Eq. (33) clearly applies whenever the gaugino masses are correlated (in any way) and trilinears (at the GUT scale) are small or correlated with the gaugino masses. As already noted, this same result also applies whenever a single term dominates in Eqs. (29) and (30). Many models fall into one or the other of these categories.

Let us reemphasize that tuning in $A_\lambda(m_Z)$ and $A_\kappa(m_Z)$ is completely unnecessary to achieve a light CP-odd Higgs boson in models with specific relations among GUT-scale parameters. Any SUSY breaking scenario that determines all soft trilinear couplings and gaugino masses from a SUSY breaking scale will automatically give $A_\lambda(m_Z) = c_\lambda M_{SUSY}$ and $A_\kappa(m_Z) = c_\kappa M_{SUSY}$, where c_λ and c_κ depend (given the known values of g_1 and g_2) only on the couplings λ , κ and λ_t (equivalently, $\tan \beta$, given the known value of m_W). The mass of the lightest CP odd Higgs boson will be given as $m_{a_1}^2 = f(\lambda, \kappa, \tan \beta) M_{SUSY}^2$ and will either be small or not. This means that, in any SUSY breaking scenario that is determined by a SUSY breaking scale only, there is no tuning of m_{a_1} with respect to the SUSY breaking scale. (Algebraically, $\frac{d \log m_{a_1}^2}{d \log M_{SUSY}^2} = 1$.) This result holds even if there are large cancellations among the RG contributions to $A_\lambda(m_Z)$ and $A_\kappa(m_Z)$. Whether or not a light CP odd Higgs boson is possible simply depends on the above couplings.

Let us now turn our attention to $\text{Br}(h_1 \rightarrow a_1 a_1)$, a completely general expression for which is the following (neglecting phase space suppression):

$$\begin{aligned} \Gamma(h_1 \rightarrow a_1 a_1) \sim & \frac{m_W^2}{32\pi g_2^2 m_{h_1}} \left[\frac{g_1^2 + g_2^2}{2} \cos 2\beta \sin(\beta + \alpha) \cos^2 \theta_A \cos \theta_S \right. \\ & \left. + 2\lambda^2 \left(\sin(\beta - \alpha) \sin^2 \theta_A \cos \theta_S + \frac{s}{v} \cos^2 \theta_A \sin \theta_S \right) \right] \end{aligned}$$

$$\begin{aligned}
& +(\cos \alpha \sin^3 \beta - \sin \alpha \cos^3 \beta) \cos^2 \theta_A \cos \theta_S) \\
& +2\lambda\kappa \left(\cos(\beta + \alpha) \sin^2 \theta_A \cos \theta_S - \sin 2\theta_A \sin \theta_S \right. \\
& \quad \left. -\frac{s}{v} \sin(\beta - \alpha) \sin 2\theta_A \cos \theta_S + \frac{s}{v} \sin 2\beta \cos^2 \theta_A \sin \theta_S \right) \\
& +\frac{\lambda A_\lambda}{v} (\sin(\beta - \alpha) \sin 2\theta_A \cos \theta_S + \sin 2\beta \cos^2 \theta_A \sin \theta_S) \\
& +\left(\frac{4\kappa^2 s}{v} - \frac{2\kappa A_\kappa}{v} \right) \sin^2 \theta_A \sin \theta_S \Big]^2
\end{aligned} \tag{35}$$

This is to be contrasted with the dominant SM decay channel, $h_1 \rightarrow b\bar{b}$, the width for which is (neglecting phase space suppression):

$$\Gamma(h_1 \rightarrow b\bar{b}) \sim \frac{3g_2^2}{32\pi m_W^2} \left(\frac{\cos \alpha}{\cos \beta} \right)^2 m_{h_1} m_b^2 \cos^2 \theta_S, \tag{36}$$

Our conventions are those of NMHDECAY in which the WW coupling relative to SM strength is given by $\sin(\beta - \alpha) \cos \theta_S$ and $v^2 = 2m_W^2/g_2^2$; m_b is to be evaluated at scale m_{h_1} . In Eq. (7), $\cos \theta_A$ gives the MSSM doublet component of the a_1 and $\sin \theta_S$ is the coefficient of the singlet component of the h_1 ; both are small numbers in our scenario. Detailed numerical results and discussion for the $h_1 \rightarrow a_1 a_1$ width will be given in the next section. However, it is important to understand the limit in which $A_\lambda, A_\kappa \rightarrow 0$. This is nicely illustrated in the case of $v/s \ll 1$. In this limit we have: $\alpha \rightarrow \beta - \pi/2$ (more precisely, $\sin(\beta - \alpha) \rightarrow \sin 2\beta + \mathcal{O}(v^2/s^2)$); $\cos \theta_A \rightarrow (v/s) \sin 2\beta + \mathcal{O}(v^3/s^3)$ (see Eq. (8)); $\sin \theta_A \rightarrow 1 - \mathcal{O}(v^2/s^2)$; $\sin \theta_S \rightarrow -(v/s)(\lambda^2/(2\kappa^2))(1 - (\kappa/\lambda) \sin 2\beta) + \mathcal{O}(v^3/s^3)$; $\cos \theta_S \rightarrow 1 - \mathcal{O}(v^2/s^2)$. With these inputs, we find

$$\begin{aligned}
\Gamma(h_1 \rightarrow a_1 a_1) & \sim \frac{m_W^2}{32\pi g_2^2 m_{h_1}} \left[2\lambda^2 + 2\lambda\kappa \sin 2\beta - \frac{4\lambda\kappa s}{v} \cos \theta_A + \frac{4\kappa^2 s}{v} \sin \theta_S + \mathcal{O}(v^2/s^2) \right]^2 \\
& \sim \frac{m_W^2}{32\pi g_2^2 m_{h_1}} [\mathcal{O}(v^2/s^2)]^2.
\end{aligned} \tag{37}$$

In particular, the $[\dots]$ does not actually vanish for $A_\lambda = A_\kappa = 0$ (there is no exact symmetry argument). One finds that $\text{Br}(h_1 \rightarrow a_1 a_1)$ can approach the $[0.1 - 0.2]$ range for the smallest κ values allowed by general theoretical consistency (good EWSB vacuum, ...) for a given λ value. This is, of course, insufficient for escaping LEP constraints when $m_{h_1} \sim 100$ GeV. Thus, having an adequate size for $\text{Br}(h_1 \rightarrow a_1 a_1)$ for escaping the LEP constraints depends critically upon having non-zero values for A_κ and, in particular, A_λ . From the numerical results presented in the next section, it will be clear that magnitudes for A_λ and A_κ of order

those developed from RGE running beginning with $A_\lambda(M_U) = A_\kappa(M_U) = 0$ are sufficient to give large $\text{Br}(h_1 \rightarrow a_1 a_1)$.

III. RESULTS

As discussed in the introduction, the Higgs sector in the NMSSM is determined by 6 basic parameters, given in Eq. (4), as well as subsidiary parameters entering through loop corrections. (In this section, all parameters are defined at scale m_Z .) Consequently, a complete survey of the parameter space is difficult. To present results in a manageable way, we fix μ and $\tan\beta$ together with all soft SUSY breaking masses and scan over trilinear and soft-trilinear couplings. We will plot results in various 2-parameter planes. The parameters are scanned over the following regions with fixed steps: $\lambda \in (0, 0.5)$ using 30 steps of size 0.01666; $\kappa \in (-0.5, 0.5)$ using 70 steps of size 0.014286; $A_\lambda \in (-300 \text{ GeV}, 300 \text{ GeV})$ using 100 steps of size 6 GeV; and finally $A_\kappa \in (-20 \text{ GeV}, 20 \text{ GeV})$ using 100 steps of size 0.4 GeV. Varying the fixed soft SUSY breaking masses does not have any significant effect on the results while different choices of μ and $\tan\beta$ lead to important changes. Thus, we will present results for several choices of μ and $\tan\beta$ keeping all SUSY-breaking masses fixed at $M_{SUSY} = 300 \text{ GeV}$. Let us recall that we are interested in looking for parameters yielding $m_{h_1} > 90 \text{ GeV}$ and $m_{a_1} < 2m_b$. The latter is imposed so that the LEP limits on $h_1 \rightarrow a_1 a_1 \rightarrow 4b$ do not apply (since if the a_1 decayed primarily to $b\bar{b}$ they would require $m_{h_1} \gtrsim 110 \text{ GeV}$, *i.e.* above our preferred $m_{h_1} \sim 100 \text{ GeV}$ value). The $m_{h_1} > 90 \text{ GeV}$ restriction implies that we are above the maximum value for which LEP limits on $h_1 \rightarrow a_1 a_1 \rightarrow 4\tau$ are available. In our plots, the small dark blue diamonds are all points that satisfy the above constraints, while the large light blue crosses are those which satisfy all experimental limits, the main experimental constraint being that $\text{Br}(h_1 \rightarrow b\bar{b})$ must be suppressed sufficiently by a large $\text{Br}(h_1 \rightarrow a_1 a_1)$ that LEP limits on the $Zh_1 \rightarrow Zb\bar{b}$ channel are satisfied. Roughly, this requires $\text{Br}(h_1 \rightarrow a_1 a_1) \gtrsim 0.7$.

We first present results for $M_{SUSY} = 300 \text{ GeV}$, $\mu = 150 \text{ GeV}$ and $\tan\beta = 10$. In Fig. 1 we plot the allowed region of parameter space in the $A_\kappa - A_\lambda$ and $\kappa - \lambda$ planes. Similarly, in Fig. 2 we plot the allowed region in the $A_\kappa - \kappa$ and $A_\lambda - \kappa$ planes. In Fig. 3, we plot a selection of the range of A_κ and A_λ values that have $m_{a_1} < 2m_b$ for fixed values of λ and κ . From Fig. 3, we see that for a given value of $A_\lambda(m_Z)$ keeping $m_{a_1} < 2m_b$ requires

that $A_\kappa(m_Z)$ be adjusted to a level of order 10%; at fixed $A_\kappa(m_Z)$, $A_\lambda(m_Z)$ must lie within about a 5% range. As quantified later, this is a rough measure of the tuning required to achieve consistency of the envisioned scenario with LEP constraints when $m_{h_1} \sim 100$ GeV. Note that A_κ, A_λ tuning could be made arbitrarily mild if very small values of $A_\kappa(m_Z)$ were allowed. However, as illustrated by the dark blue points, too small a value for $A_\kappa(m_Z)$ leads to a value for $\text{Br}(h_1 \rightarrow a_1 a_1)$ that is small and therefore a value of $\text{Br}(h_1 \rightarrow b\bar{b})$ that is too large for consistency with LEP constraints on the $Zh \rightarrow Zb\bar{b}$ channel. In any case, as we have discussed, very small values of $A_\kappa(m_Z)$ and $A_\lambda(m_Z)$ would be purely accidental from the RGE point of view.

The correlations between $A_\kappa(m_Z)$ and $A_\lambda(m_Z)$ required to achieve $m_{a_1} < 2m_b$ can be understood from Eqs. (12)–(19). For the following discussion, we consider the case of $\mu > 0$, implying $s > 0$. Clearly, in order for both eigenvalues of the CP-odd Higgs mass matrix squared to be positive, both diagonal elements have to be positive. In the limit $|A_\kappa| \ll |A_\lambda| \sim v \ll s$, and $\tan\beta \gtrsim \text{few}$, M_{22}^2 is dominated by the last term (unless $|A_\kappa|$ is too small), and so $M_{22}^2 > 0$ leads to the condition $\kappa A_\kappa < 0$. This means that the contribution of the κA_κ term to the mass of the lightest CP-odd Higgs is positive, see Eqs. (9) and (19). Next, we note that $M_{11}^2 > 0$ requires $A_\lambda + \kappa s > 0$. Given that $\kappa A_\kappa < 0$, this implies that the denominator of the first term in the $m_{a_1}^2$ expression given in Eq. (19) is positive, and that this first term will therefore have the same sign as κA_λ . Thus, in order for the terms proportional to κA_λ and $-\kappa A_\kappa$ in Eq. (19) to cancel so as to give small $m_{a_1}^2$, κA_λ must have the same sign as κA_κ . Given that $\kappa A_\kappa < 0$, we must therefore also have $\kappa A_\lambda < 0$. Altogether, we have two disconnected regions of allowed parameter space. The first one is for $\kappa > 0$, $A_\lambda < 0$ and $A_\kappa < 0$. It is the largest region because the condition $A_\lambda + \kappa s > 0$ is easily satisfied, especially with smaller values of A_λ . The second region is for $\kappa < 0$, $A_\lambda > 0$ and $A_\kappa > 0$ which is further constrained by $A_\lambda + \kappa s > 0$ and thus requires larger values of A_λ and consequently larger values of A_κ .

The above discussion is not valid when A_κ is so small that the κA_κ term does not dominate M_{22}^2 . For such parameters, $m_{a_1} < 2m_b$ can still be achieved, but $\text{Br}(h_1 \rightarrow a_1 a_1) > 0.7$ is not possible. This region is seen in Fig. 2 as a large dark (blue) region with a large range of $A_\lambda > 0$ with $\kappa > 0$ in the right-hand plot and a narrow band of very small A_κ values and $\kappa > 0$ in the left-hand plot. For this region, $\lambda < 0.1$ is typical. This region can be

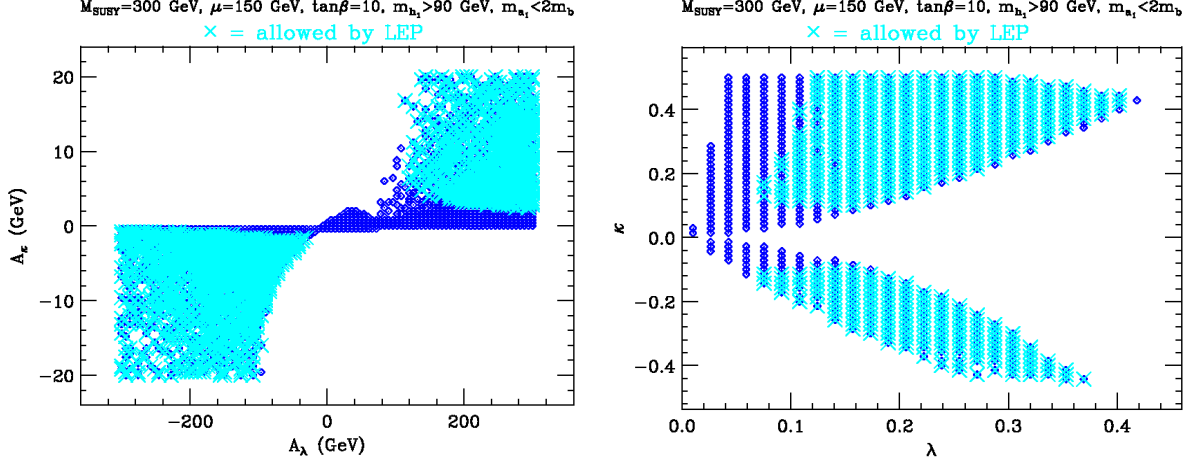


FIG. 1: Allowed parameter space in the $A_\kappa - A_\lambda$ and $\kappa - \lambda$ planes. Light grey (cyan) large crosses are points that satisfy all experimental limits. The dark (blue) diamonds are those points that do not have large enough $\text{Br}(h_1 \rightarrow a_1 a_1)$ so as to suppress $\text{Br}(h_1 \rightarrow b\bar{b})$ sufficiently to escape LEP limits.

understood by noting that when κA_κ is negligible, then Eq. (19) reduces to

$$m_{a_1}^2 \xrightarrow{A_\kappa \rightarrow 0} \frac{9A_\lambda \kappa \lambda v^2 \sin 2\beta}{2(A_\lambda + \kappa s)}. \quad (38)$$

Since we require both $m_{a_1}^2 > 0$ and $M_{11}^2 \propto (A_\lambda + \kappa s) > 0$, see Eq. (12), we must have $A_\lambda > 0$ and $\kappa > 0$. Small $m_{a_1}^2$ is easily achieved in a variety of ways, for example if A_λ is small compared to κs or, more generally, for small λA_λ and large $\tan \beta$. Radiative corrections play a significant role also, reducing the tree-level prediction given above by a substantial amount.

The dependence of the branching ratio for $h_1 \rightarrow a_1 a_1$ on A_κ and A_λ is given in Fig. 4. As we have stressed, a large value for $\text{Br}(h_1 \rightarrow a_1 a_1)$ is crucial for an $m_{h_1} \sim 100$ GeV light SM-like Higgs to have escaped LEP constraints. (It is the constraint $m_{a_1} < 2m_b$ which guarantees that when $A_\kappa \sim 0$ then λA_λ must be very small as well, and vice versa, thereby implying small $\text{Br}(h_1 \rightarrow a_1 a_1)$.) It is interesting to see that if $|A_\kappa| \gtrsim 2$ GeV and $|A_\lambda| \gtrsim 30$ GeV (as typical for the sizes of the RGE-induced contributions) then $\text{Br}(h_1 \rightarrow a_1 a_1)$ is almost always large enough for the h_1 to have escaped detection through the $h_1 \rightarrow b\bar{b}$ channel. These plots also show clearly that $\text{Br}(h_1 \rightarrow a_1 a_1)$ approaches a small (most typically, extremely small) value when $A_\kappa, A_\lambda \rightarrow 0$. This suppression was discussed analytically in the small v/s limit in the previous section.

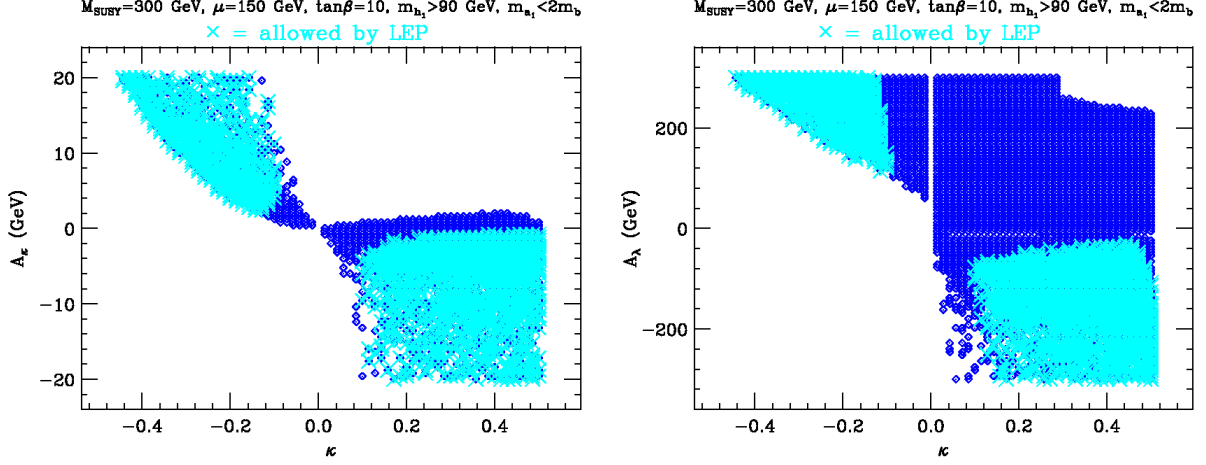


FIG. 2: Allowed parameter space in the $A_\kappa - \kappa$ and $A_\lambda - \kappa$ planes. Point conventions as in Fig. 1.

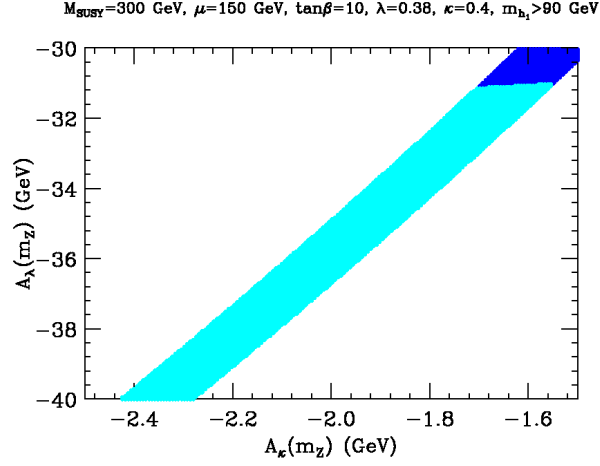


FIG. 3: A selected region of the allowed parameter space in the $A_\kappa - A_\lambda$ plane for fixed values of $\lambda = 0.38$ and $\kappa = 0.4$. Point conventions as in Fig. 1.

Another way of characterizing the limited allowed region in A_κ and A_λ for which m_{a_1} stays below $2m_b$ (shown in Fig. 3), is to calculate the tuning [as defined in Eq. (23)] of A_λ and A_κ necessary to achieve this situation. The dependence of F_{MAX} on A_κ and A_λ is given in Fig. 5. Similarly, the dependence of F_{MAX} on κ and λ is given in Fig. 6. As expected, the smallest fine tuning or sensitivity is achieved for as small A_κ and A_λ as possible. Of course, as we discussed earlier, very small values of A_κ and A_λ would require cancellations between the bare values and the RGE-induced radiative corrections and this kind of cancellation would not be visible from the definition of F_{MAX} given in Eq. (23). However, this is not a particularly worrisome point given that, as discussed with regard to Fig. 4, very small values

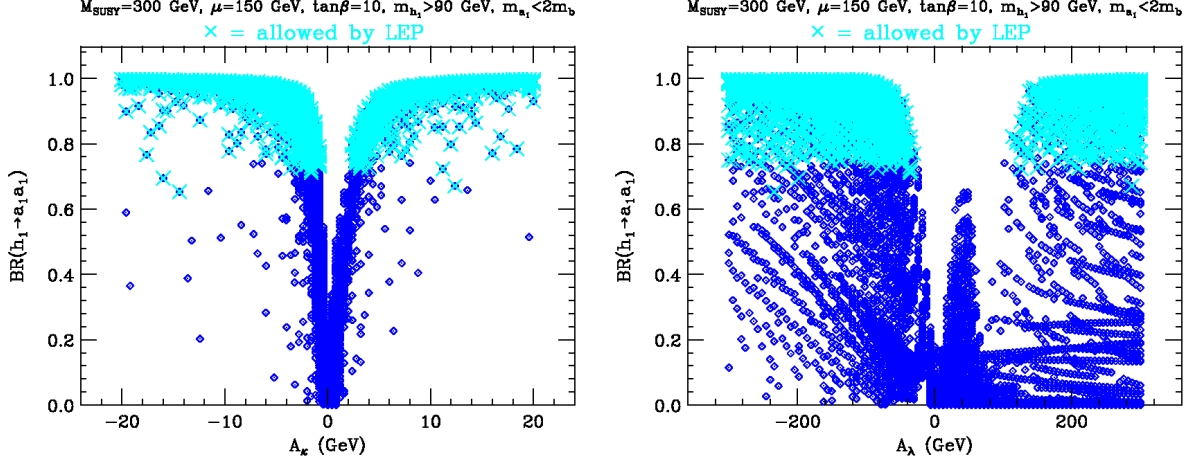


FIG. 4: $\text{Br}(h_1 \rightarrow a_1 a_1)$ vs. A_κ and A_λ for $\mu = 150$ GeV and $\tan\beta = 10$. Point conventions as in Fig. 1.

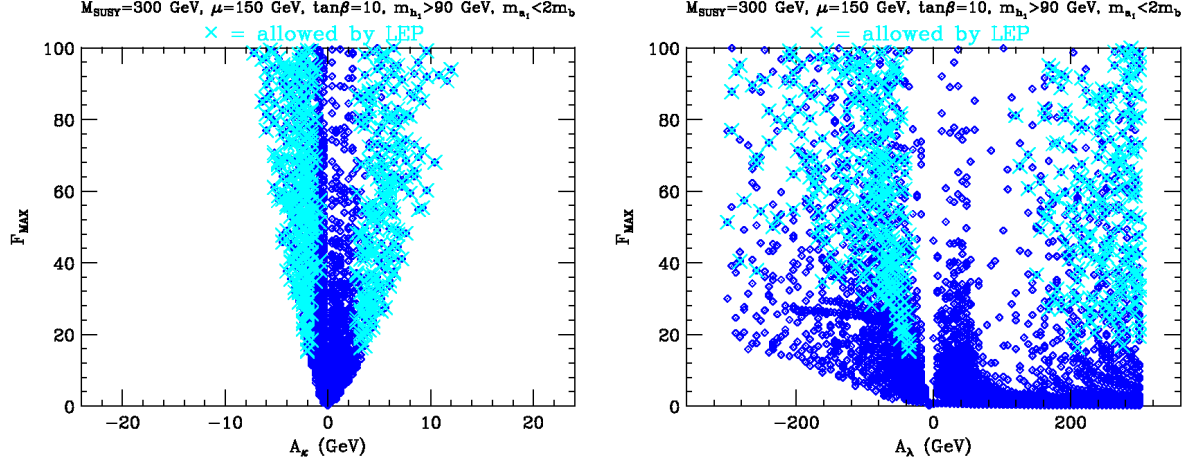


FIG. 5: Tuning in $m_{a_1}^2$ vs. A_κ and A_λ . Point conventions as in Fig. 1.

of A_κ and A_λ do not in any case lead to large enough $\text{Br}(h_1 \rightarrow a_1 a_1)$ that $\text{Br}(h_1 \rightarrow b\bar{b})$ is adequately suppressed. Thus, in the region of parameter space where soft trilinear couplings are at least of order the typical RGE-induced contributions, which is also the region where $\text{Br}(h_1 \rightarrow a_1 a_1)$ is large, the F_{MAX} measure of the tuning of the soft trilinear couplings can be as small as $\mathcal{O}(5\% - 10\%)$.

However, as discussed in the analytic section of the paper, fine-tuning with respect to GUT-scale parameters, denoted there as $F_{m_{a_1}}$, need not be as large as F_{MAX} . In particular, there are many model scenarios in which $F_{m_{a_1}}$ is reduced compared to F_{MAX} by cancellations between the dependence of $A_\lambda(m_Z)$ on the dominant GUT-scale parameter p and the de-

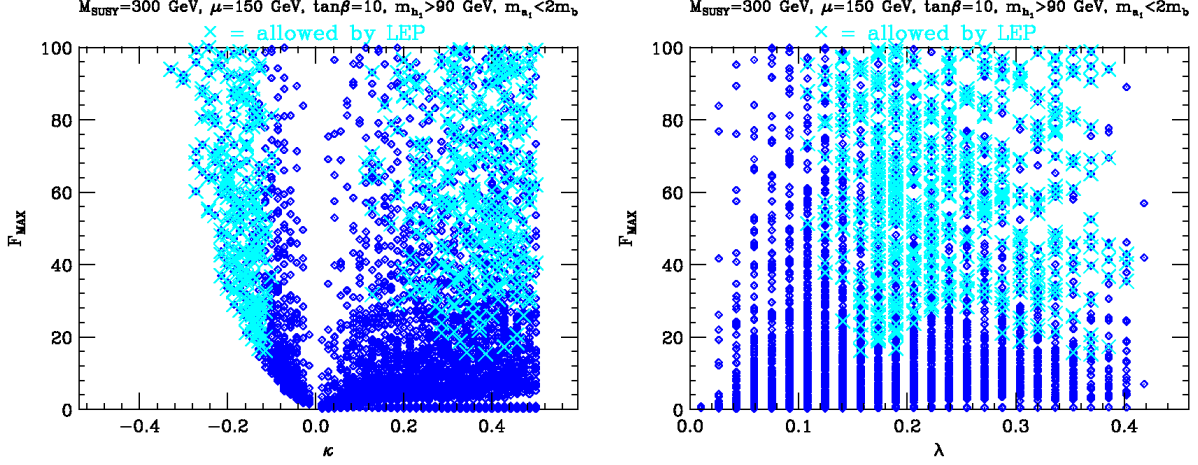


FIG. 6: Tuning in $m_{a_1}^2$ vs. κ and λ . Point conventions as in Fig. 1.

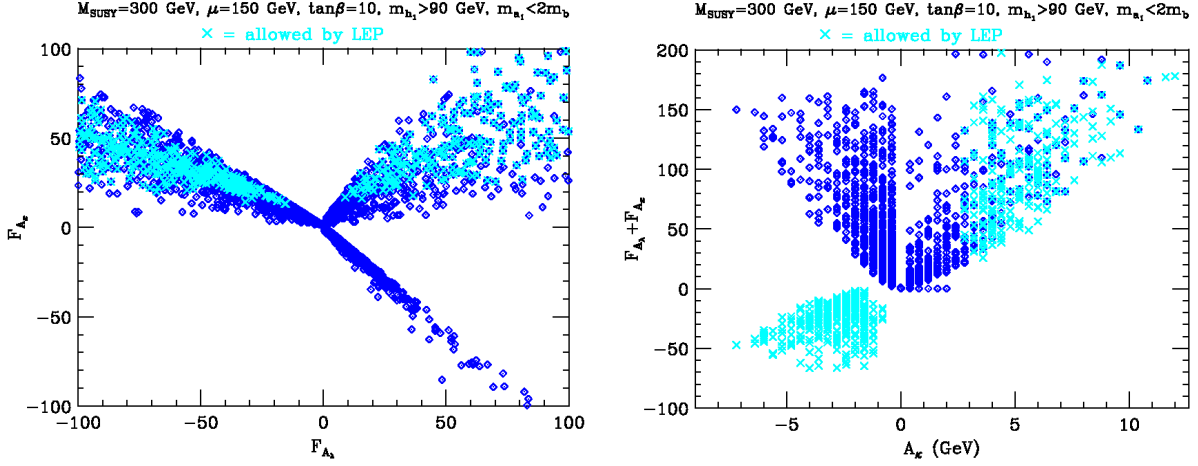


FIG. 7: In the left-hand frame, we plot F_{A_κ} vs. F_{A_λ} for the points with $F_{MAX} < 100$. In the right-hand frame, we plot $F_{A_\lambda} + F_{A_\kappa}$ vs. A_κ for these same points.

pendence of $A_\kappa(m_Z)$ on this same p , in the simplest cases yielding $F_{m_{a_1}} \sim F_{A_\lambda} + F_{A_\kappa}$. In the most naive approximation, $m_{a_1}^2$ is linear in A_λ and linear in A_κ and therefore $F_{A_\lambda} \sim -F_{A_\kappa}$ and $F_{m_{a_1}}$ is then quite small. Thus, it is important to understand the correlations between F_{A_λ} and F_{A_κ} in order to assess the extent to which $F_{A_\lambda} + F_{A_\kappa}$ can be small. In the left-hand window of Fig. 7, we plot F_{A_κ} vs. F_{A_λ} for points with $F_{MAX} < 100$. We see that many of the points have $F_{A_\lambda} \sim -F_{A_\kappa}$. The corresponding values of $F_{A_\lambda} + F_{A_\kappa}$ appear in the right-hand plot. We observe that the LEP-allowed points with small negative A_κ (which are those with the smallest magnitudes of F_{A_λ} and F_{A_κ} separately) yield still smaller $F_{A_\lambda} + F_{A_\kappa}$ and therefore possibly very small $F_{m_{a_1}}$ for appropriate GUT-scale models. For all LEP-allowed

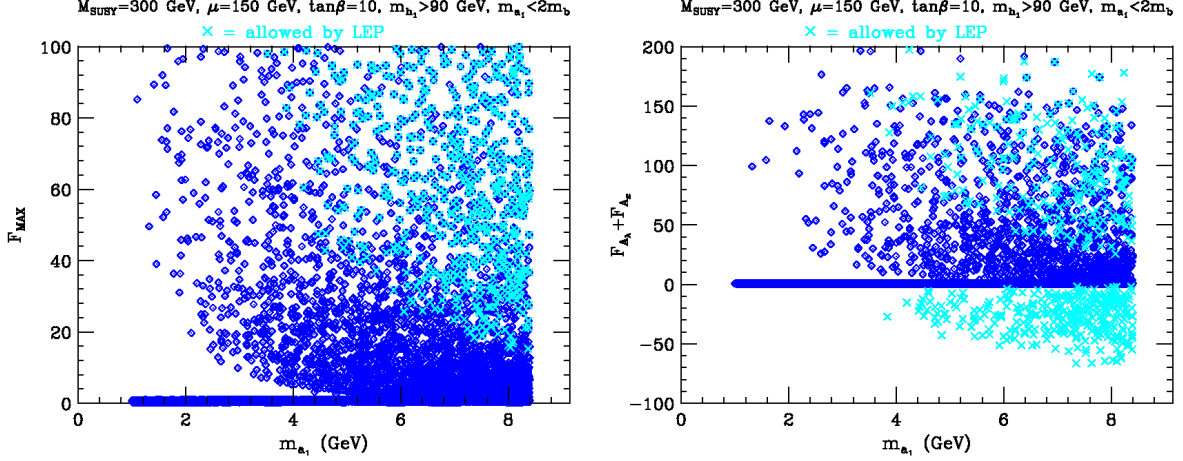


FIG. 8: In the left-hand frame, we plot F_{MAX} vs. m_{a_1} for the points with $F_{MAX} < 100$. In the right-hand frame, we plot $F_{A_\lambda} + F_{A_\kappa}$ vs. m_{a_1} for these same points.

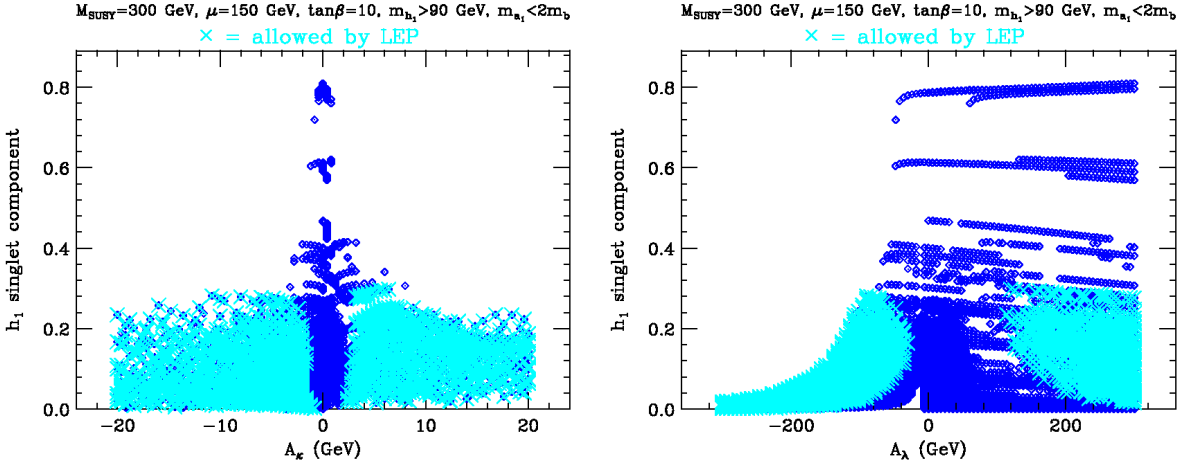


FIG. 9: Singlet component of h_1 vs. A_κ and A_λ . Point conventions as in Fig. 1.

$A_\kappa < 0$ points, $F_{A_\lambda} + F_{A_\kappa}$ is much smaller than F_{MAX} .

It is also useful to understand the extent to which F_{MAX} and $F_{A_\lambda} + F_{A_\kappa}$ depend on m_{a_1} . This dependence is revealed in Fig. 8. We see that the smallest F_{MAX} values are achieved for the larger m_{a_1} values up near $2m_b$. Small values of $F_{A_\lambda} + F_{A_\kappa}$ are distributed over the broader range of $4 \text{ GeV} \lesssim m_{a_1} < 2m_b$. In either case, the fine-tuning associated with $m_{a_1} < 2m_b$ suggests some preference for $m_{a_1} > 2m_\tau$. This is important in that $h_1 \rightarrow a_1 a_1 \rightarrow 4\tau$ decays may prove to be visible at the LHC, whereas $h_1 \rightarrow a_1 a_1$ with $a_1 \rightarrow c\bar{c}, gg, \dots$ will be much harder to detect.

Higgs phenomenology is crucially dependent upon the singlet and doublet compositions of

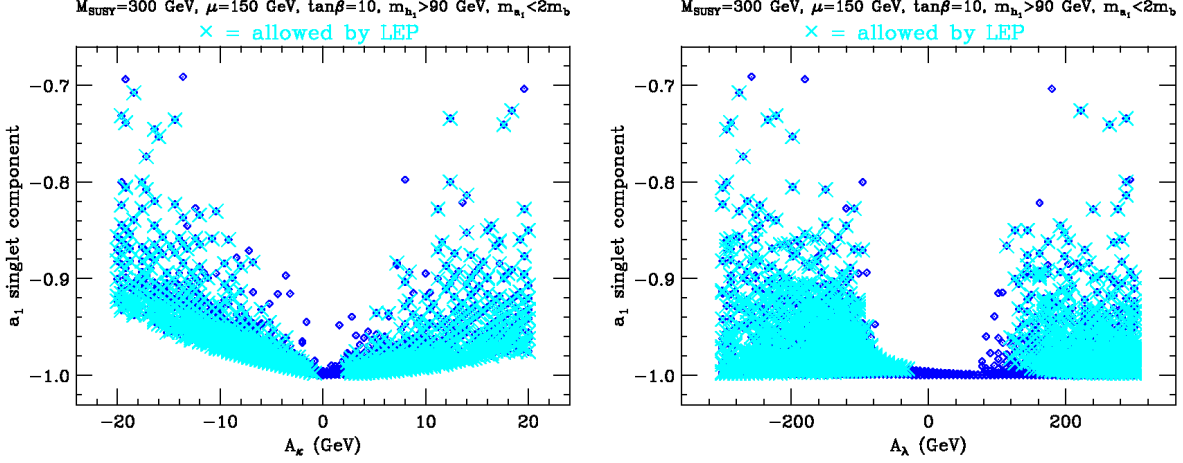


FIG. 10: Singlet component of a_1 vs. A_κ and A_λ . Point conventions as in Fig. 1.

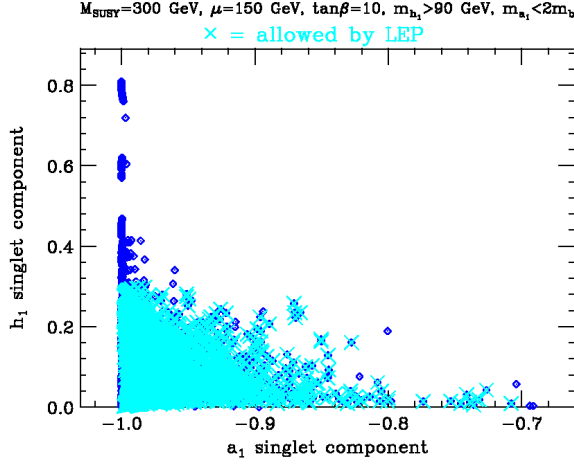


FIG. 11: Singlet component of h_1 vs. singlet component of a_1 . Point conventions as in Fig. 1.

the lightest CP-even and CP-odd Higgs mass eigenstates. The lightest CP-even Higgs boson is preferably SM-like although it can have up to 20 % singlet component, see Fig. 9, while the lightest CP-odd Higgs boson has to be very close to being a singlet, at least 98 % singlet in the region where the least tuning is necessary, see Fig. 10. (Here, $\sin\theta_A$, see Eq. (7), is the singlet component of the a_1 at the amplitude level. The *probability* for the a_1 to be singlet is $\sin^2\theta_A$. Similar definitions are used in the case of the h_1 .) This correlation between the h_1 and a_1 compositions is explicit in the plot of the h_1 singlet component versus the a_1 singlet component given in Fig. 11. This figure shows that as the a_1 becomes less singlet the h_1 must have less singlet component. The left-hand plot of Fig. 12 also makes it clear that the h_1 singlet component must be small (or zero) in order to maximize $\text{Br}(h_1 \rightarrow a_1 a_1)$.

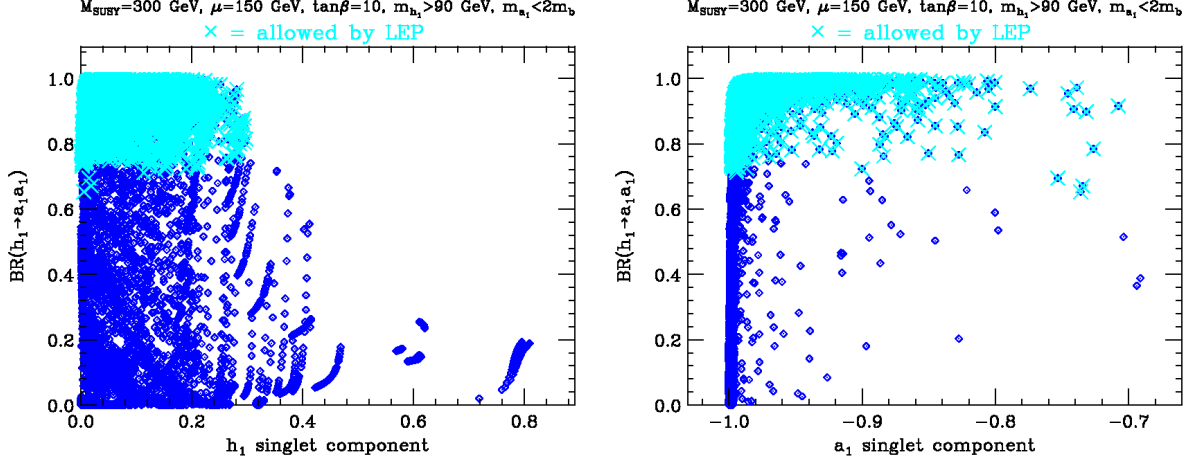


FIG. 12: $Br(h_1 \rightarrow a_1 a_1)$ vs. singlet component of h_1 and a_1 . Point conventions as in Fig. 1.

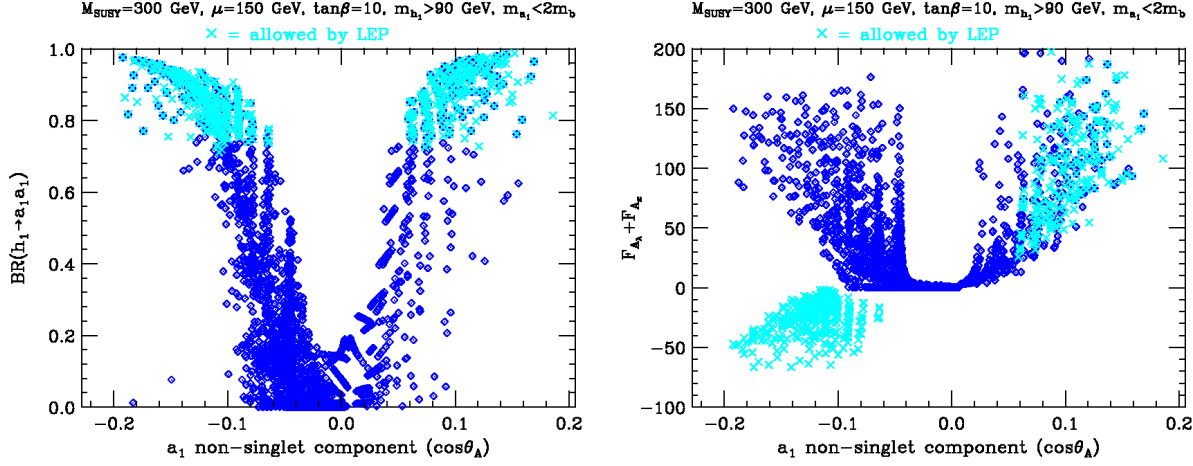


FIG. 13: $Br(h_1 \rightarrow a_1 a_1)$ and $F_{A_\kappa} + F_{A_\lambda}$ vs. the non-singlet component of the a_1 . Point conventions as in Fig. 1.

The right-hand plot of Fig. 12 shows that the a_1 singlet component must be at least 70% in amplitude, *i.e.* 50% in probability, for the range of parameters scanned with most points corresponding to an a_1 that is mainly singlet.

A particularly revealing pair of plots are those of Fig. 13 where we show how $Br(h_1 \rightarrow a_1 a_1)$ and $F_{A_\kappa} + F_{A_\lambda}$ depend on $\cos \theta_A$, the non-singlet component of the a_1 . We see from the first plot that there is a lower bound on $|\cos \theta_A|$ of order 0.06 (this is the bound for $\tan \beta = 10$ — the precise number depends on $\tan \beta$) in order for $Br(h_1 \rightarrow a_1 a_1)$ to be large enough that LEP limits are evaded. The existence of the lower bound follows from the fact, discussed earlier, that κ and A_λ must have opposite signs in order for the scenario to be

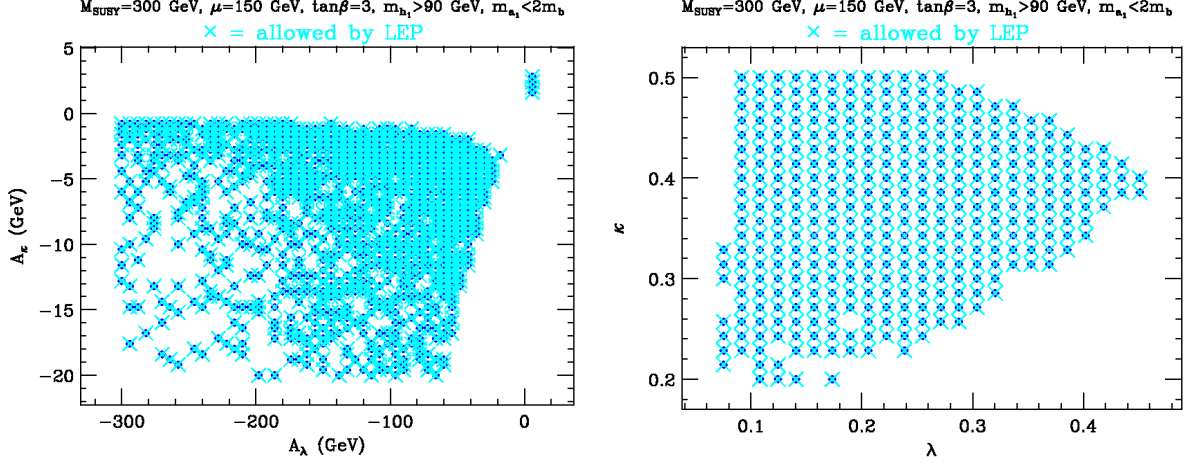


FIG. 14: Allowed parameter space in the $A_\kappa - A_\lambda$ and $\kappa - \lambda$ planes for $\tan \beta = 3$ and $\mu = 150$ GeV. Point conventions as in Fig. 1.

viable. Since, the non-singlet component of the a_1 is proportional to $A_\lambda - 2\kappa s$, see Eq. (22), it cannot go to zero for the given correlation of signs. From the second plot, we see that the $F_{A_\kappa} + F_{A_\lambda}$ measure of fine tuning for m_{a_1} has a very distinct minimum value close to 0 for $\cos \theta_A \sim -0.1$. Combined with the dependence of $F_{A_\kappa} + F_{A_\lambda}$ on m_{a_1} displayed in Fig. 8, we see a possible preference for $m_{a_1} > 2m_\tau$ and $\cos \theta_A \sim -0.1$ in order to be reasonably certain that fine-tuning is not required in order to achieve large $\text{Br}(h_1 \rightarrow a_1 a_1)$ and $m_{a_1} < 2m_b$. We note that the coupling of the a_1 to down type quarks is proportional to $\tan \beta \cos \theta_A$ which is never smaller than about 0.6 in magnitude for the points that escape LEP limits. Thus, even though the a_1 is largely singlet, it has substantial down-quark and lepton couplings. In a follow-up paper [19], we show that this implies an m_{a_1} -dependent lower limit on the branching ratio for $\Upsilon \rightarrow \gamma a_1$ decays. This lower limit can probably be probed at future, if not existing, B factories if m_{a_1} is not too close to M_Υ , especially if $m_{a_1} > 2m_\tau$ so that $a_1 \rightarrow \tau^+ \tau^-$ decays are dominant.

Finally, in order to see the effect of varying $\tan \beta$ and μ , we give a selection of some of the same plots for: $\mu = 150$ GeV and $\tan \beta = 3$; $\mu = 150$ GeV and $\tan \beta = 50$; and $\mu = 400$ GeV with $\tan \beta = 10$. These appear in Figs. 14 — 23. We note that there is an exact symmetry under $\mu \rightarrow -\mu$ (implying $s \rightarrow -s$ in the $\lambda > 0$ convention we employ), $A_\kappa \rightarrow -A_\kappa$ and $A_\lambda \rightarrow -A_\lambda$. Thus, only positive μ values need be considered when both signs of A_λ and A_κ are scanned.

Comparing the plots for $\tan \beta = 3$, Figs. 14 — 16, and the plots for $\tan \beta = 50$, Figs. 17

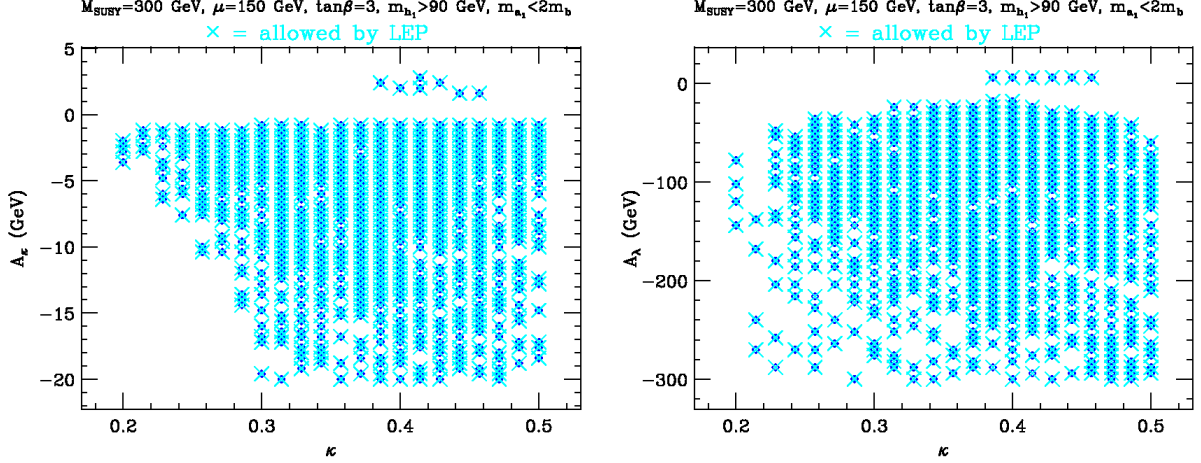


FIG. 15: Allowed parameter space in the $A_\kappa - \kappa$ and $A_\lambda - \kappa$ planes for $\tan \beta = 3$ and $\mu = 150$ GeV. Point conventions as in Fig. 1.

– 19, with the previous plots for $\tan \beta = 10$ we see that the region of allowed parameter space for $\kappa > 0$, $A_\lambda < 0$ and $A_\kappa < 0$ does not change much when varying $\tan \beta$. On the other hand the allowed region of parameter space with $\kappa < 0$, $A_\lambda > 0$ and $A_\kappa > 0$ changes dramatically. It does not even exist for $\tan \beta = 3$ ⁴. The reason is that the first two terms in Eq. (14) are less suppressed for smaller $\tan \beta$ and they combine into a term proportional to $A_\lambda + 4\kappa s$. The last term in Eq. (14) dominates only for larger values of A_κ . If the last term does not dominate, the first two terms are positive only for very large A_λ making the region with $\kappa < 0$, $A_\lambda > 0$ and $A_\kappa > 0$ very constrained. For exactly the same reason, this region is larger for $\tan \beta = 50$ compared to $\tan \beta = 10$ and the allowed parameter space expands to lower values of A_κ as particularly noticeable in the A_κ vs. κ plots; compare Figs. 18, 15 and 2. In the region of parameter space with $\kappa > 0$, $A_\lambda < 0$ and $A_\kappa < 0$ the condition $A_\lambda + 4\kappa s > 0$ is always satisfied when the necessary condition for having positive mass squared eigenvalues, $A_\lambda + \kappa s > 0$, is satisfied. Therefore, this region of parameter space is not very sensitive to $\tan \beta$.

Quite interestingly, once $m_{a_1} < 2m_b$ is achieved for $\tan \beta = 3$, $\text{Br}(h_1 \rightarrow a_1 a_1)$ is automatically large enough ($\gtrsim 0.75$ for the most part) and, correspondingly, $\text{Br}(h_1 \rightarrow b\bar{b})$ is sufficiently suppressed that $Zh \rightarrow Zb\bar{b}$ constraints at LEP are satisfied; see Fig. 16. As in

⁴ There is a tiny allowed region with positive A_κ and positive but very small A_λ . This region is not a continuation of the region present in the plots for $\tan \beta = 10$.

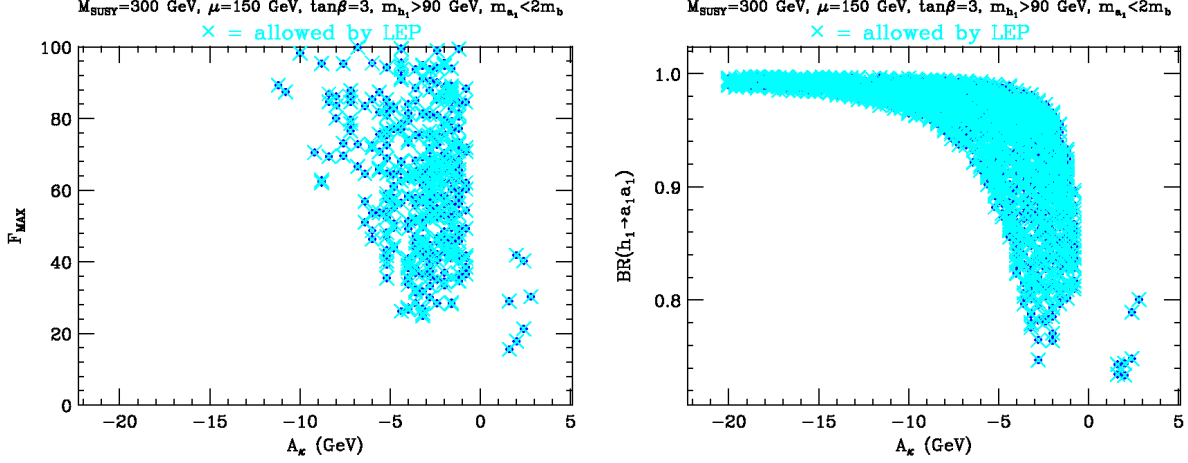


FIG. 16: F_{MAX} and $\text{Br}(h_1 \rightarrow a_1 a_1)$ vs. A_κ for $\tan \beta = 3$ and $\mu = 150$ GeV. Point conventions as in Fig. 1.

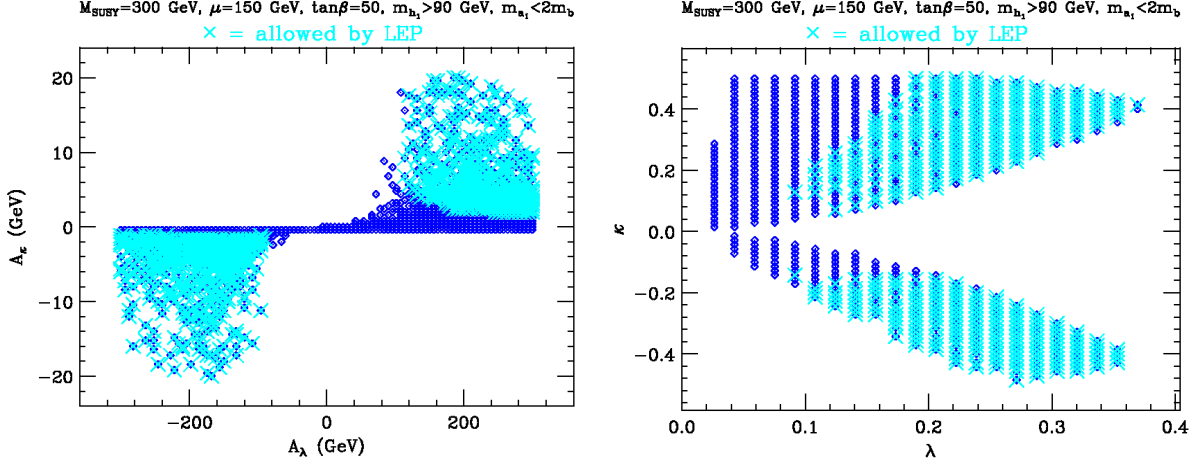


FIG. 17: Allowed parameter space in the $A_\kappa - A_\lambda$ and $\kappa - \lambda$ planes for $\tan \beta = 50$ and $\mu = 150$ GeV. Point conventions as in Fig. 1.

the $\tan \beta = 10$ case, F_{MAX} is smallest for the smallest possible A_κ and approaches ~ 15 for a couple of the points with $A_\kappa > 0$. Overall, it would appear that $m_{a_1} < 2m_b$ is a bit more difficult to achieve without tuning when $\tan \beta = 3$ vs. when $\tan \beta = 10$. For $\tan \beta = 50$, see Fig. 19, small F_{MAX} ($\lesssim 20$) is achieved for a narrower range of A_κ and $A_\kappa > 0$ gives the smallest F_{MAX} values (whereas for $\tan \beta = 10$ there was no particular preference with regard to the sign of A_κ).

Finally, we discuss the effect of increasing μ . We consider $\mu = 400$ GeV at $\tan \beta = 10$ and present results in Figs. 20 — 23. These figures clearly show that the range of parameter space

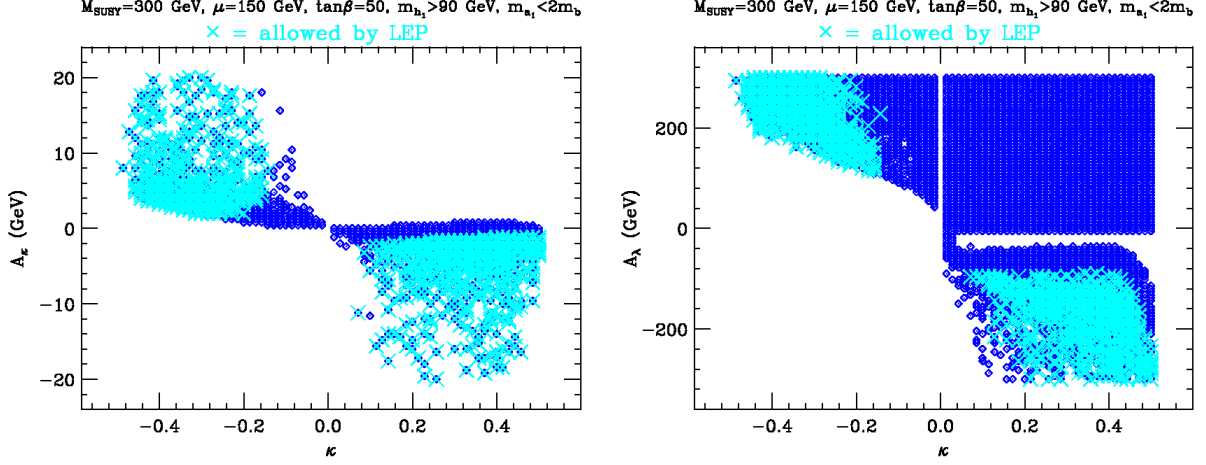


FIG. 18: Allowed parameter space in the $A_\kappa - \kappa$ and $A_\lambda - \kappa$ planes for $\tan \beta = 50$ and $\mu = 150$ GeV. Point conventions as in Fig. 1.

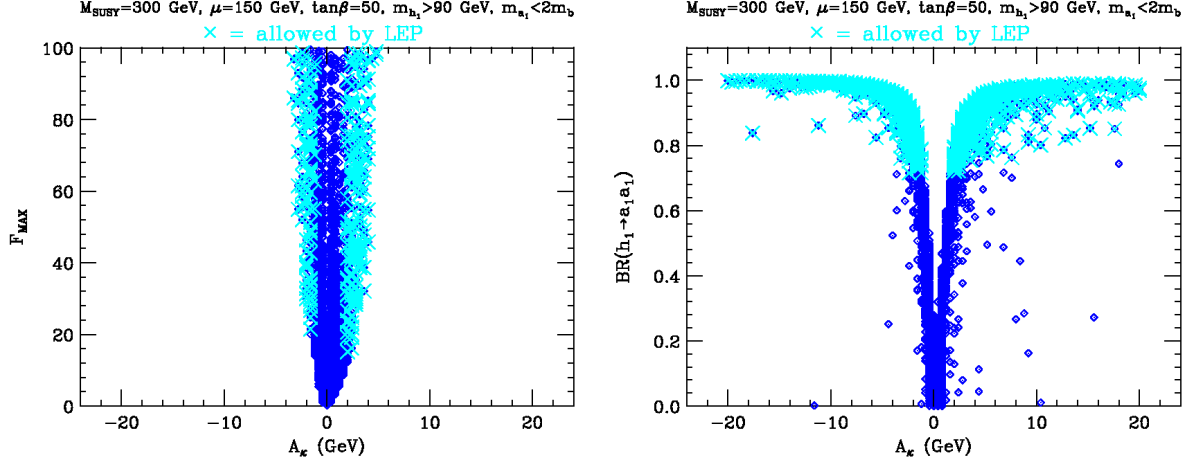


FIG. 19: F_{MAX} and $\text{Br}(h_1 \rightarrow a_1 a_1)$ vs. A_κ for $\tan \beta = 50$ and $\mu = 150$ GeV. Point conventions as in Fig. 1.

for which $m_{a_1} < 2m_b$ shrinks with increasing μ . This is easy to understand from Eq. (9) or Eq. (19). For fixed λ , increasing μ results in an increase of s . Consequently the term proportional to A_λ in the formula for m_{a_1} is further suppressed while the term proportional to A_κ is enhanced. In order to compensate for this so as to keep m_{a_1} small, smaller values of κ and A_κ and larger values of λ and A_λ are required as compared to the $\mu = 150$ GeV case. Moreover, the $m_{a_1} < 2m_b$ region of parameter space with $\kappa < 0$, $A_\lambda > 0$ and $A_\kappa > 0$ is even further constrained by the condition $A_\lambda + \kappa s > 0$ which requires larger A_λ for larger s . These effects are clearly visible in Fig. 20 and Fig. 21. The increased value of A_λ required for this

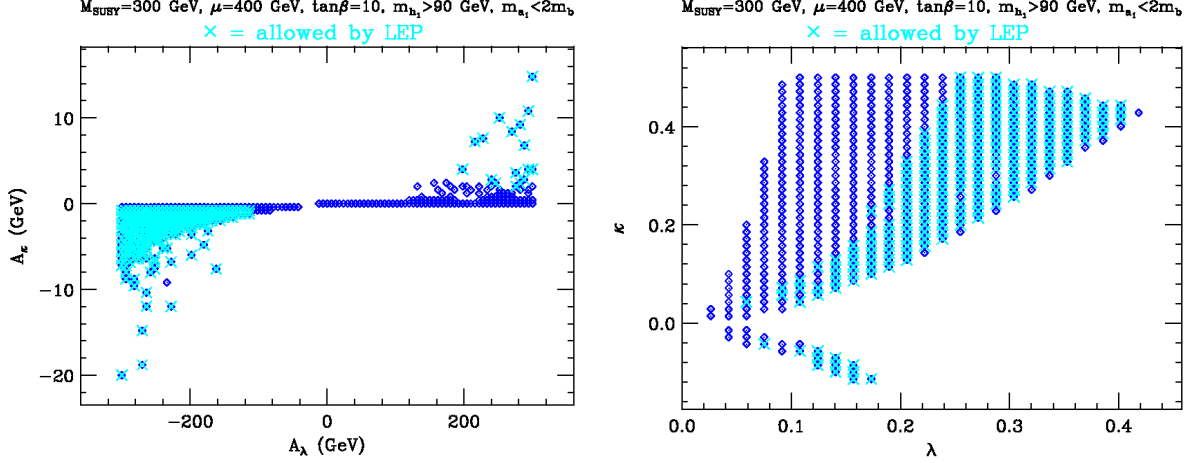


FIG. 20: Allowed parameter space in the $A_\kappa - A_\lambda$ and $\kappa - \lambda$ planes for $\tan\beta = 10$ and $\mu = 400$ GeV. Point conventions as in Fig. 1.

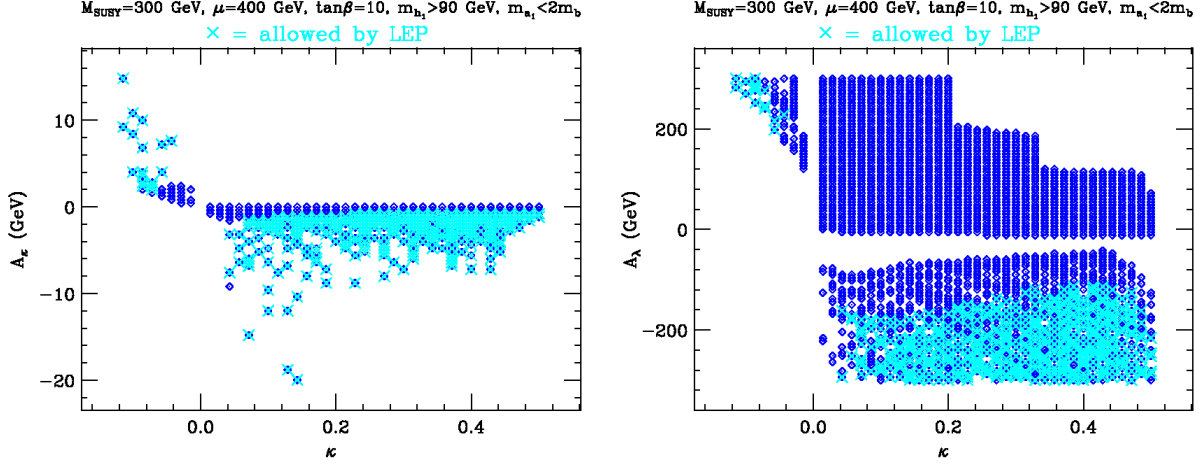


FIG. 21: Allowed parameter space in the $A_\kappa - \kappa$ and $A_\lambda - \kappa$ planes for $\tan\beta = 10$ and $\mu = 400$ GeV. Point conventions as in Fig. 1.

scenario to work for larger μ leads to larger tuning necessary to achieve $m_{a_1} < 2m_b$. Fig. 22 shows a dramatic narrowing of the A_κ region for which moderate F_{MAX} values are achieved and that the best F_{MAX} value for points having large enough $\text{Br}(h_1 \rightarrow a_1 a_1)$ that LEP limits are evaded is of order ~ 30 in contrast to the $F_{MAX} \sim 15$ values achieved for $\mu = 150$ GeV. However, we see from Fig. 23 that the values of F_{A_λ} and F_{A_κ} are more strongly correlated so that $F_{A_\lambda} + F_{A_\kappa}$ can again take on small values. As we have seen, the latter implies small $F_{m_{a_1}}$ in models in which the soft-SUSY breaking parameters are correlated or $A_\lambda(m_Z)$ and $A_\kappa(m_Z)$ are dominated by a single soft-SUSY-breaking parameter.

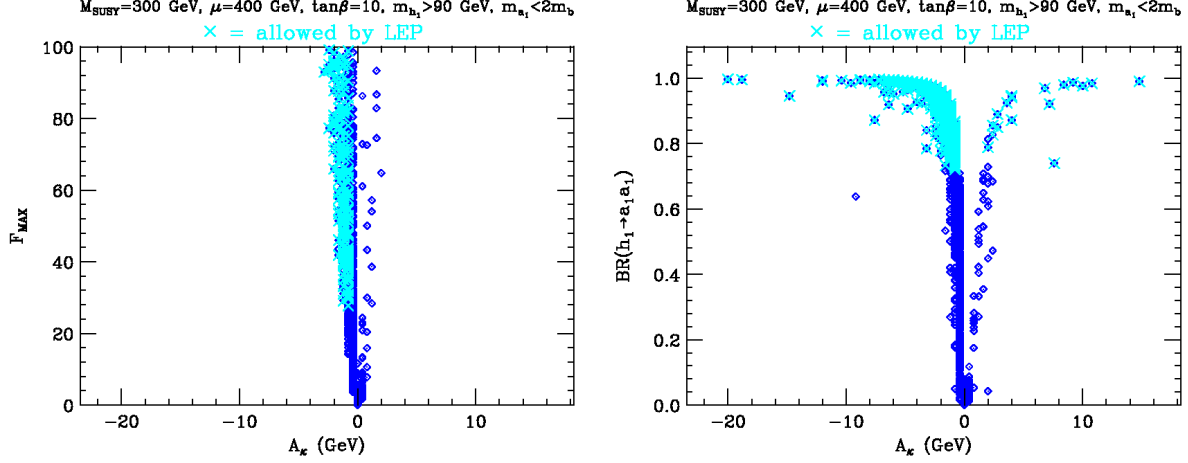


FIG. 22: F_{MAX} and $\text{Br}(h_1 \rightarrow a_1 a_1)$ vs. A_κ for $\tan \beta = 10$ and $\mu = 400$ GeV. Point conventions as in Fig. 1.

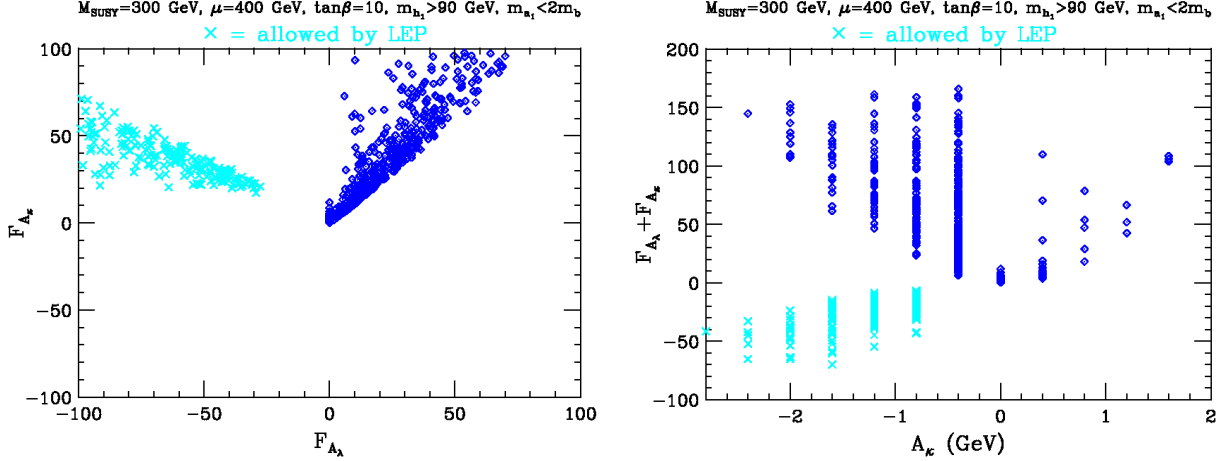


FIG. 23: We plot F_{A_κ} vs. F_{A_λ} (left window) and $F_{A_\kappa} + F_{A_\lambda}$ vs. A_κ (right window) for $\mu = 400$ GeV, and $\tan \beta = 10$. Point conventions as in Fig. 1.

Given that detection of the h_1 at hadron colliders will be quite challenging for the large- $\text{Br}(h_1 \rightarrow a_1 a_1)$ scenarios that we focus on, an interesting question is then whether or not the other Higgs bosons $h_{2,3}$ and a_2 might be detectable. This will depend on their masses and on their couplings. We will see that within the scenarios considered, their masses can range from somewhat above 100 GeV to quite large values. As regards their couplings, since the h_1 has quite SM-like WW, ZZ couplings for the scenarios being considered (as illustrated earlier), the $h_{2,3}$ will have quite weak WW, ZZ couplings, and of course the a_2 has no tree-level couplings to WW, ZZ . Thus, the question is whether production mechanisms relying

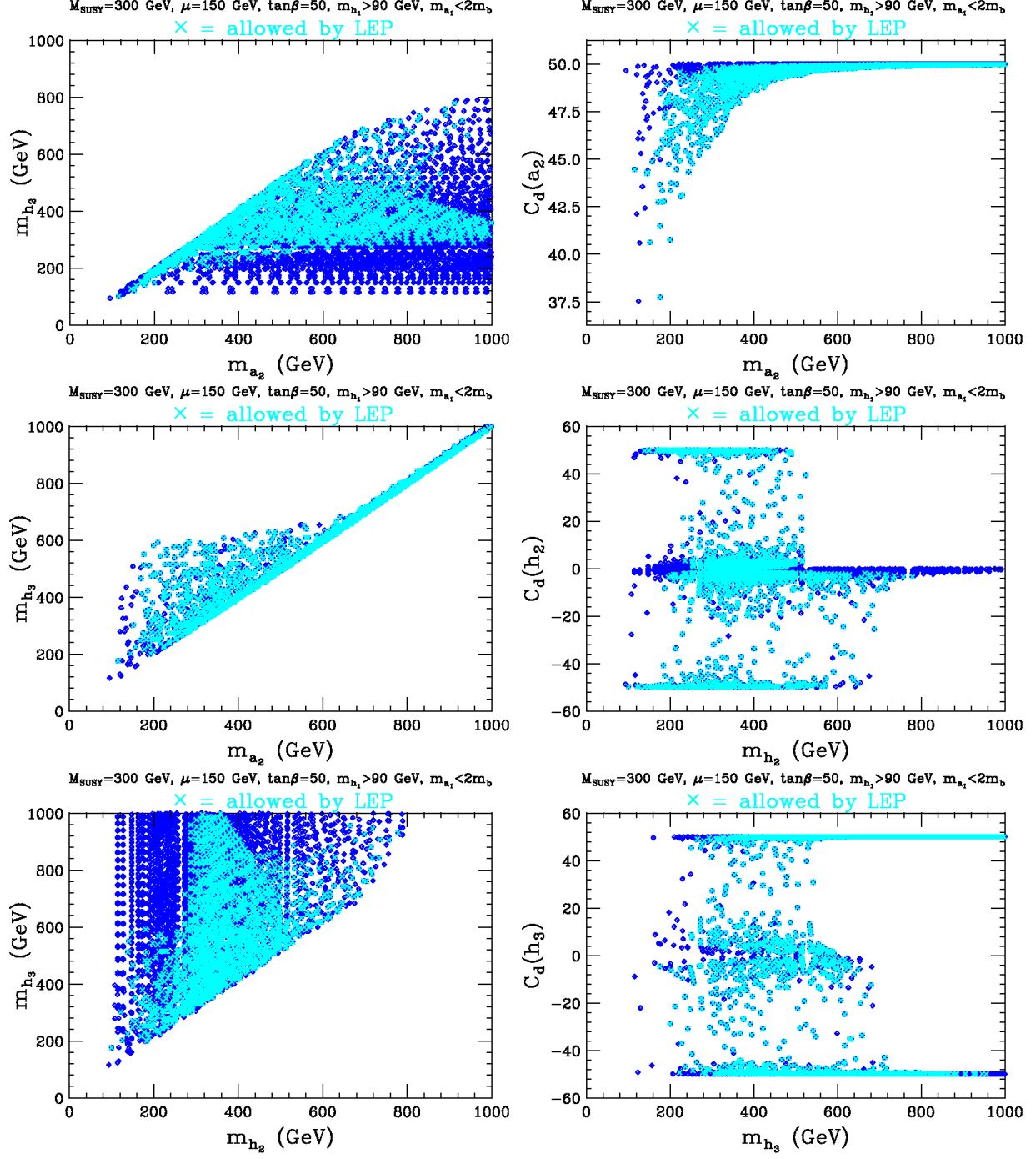


FIG. 24: In the left-hand set of plots, we present m_{h_2} vs. m_{a_2} (top), m_{h_3} vs. m_{a_2} (middle) and m_{h_3} vs. m_{h_2} (bottom). In the right-hand set of plots, we present $C_d(a_2)$ vs. m_{a_2} (top), $C_d(h_2)$ vs. m_{h_2} (middle) and $C_d(h_3)$ vs. m_{h_3} (bottom). All plots are for $\tan\beta = 50$ and $\mu = 150$ GeV. Point conventions as in Fig. 1.

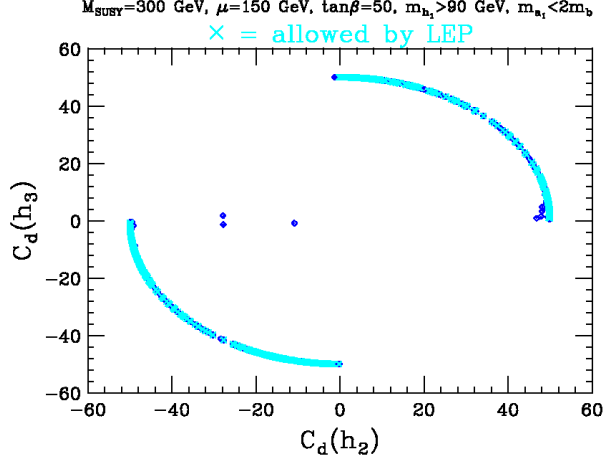


FIG. 25: We plot $C_d(h_3)$ vs. $C_d(h_2)$ for $\tan\beta = 50$ and $\mu = 150$ GeV. Point conventions as in Fig. 1.

on $q\bar{q}$ couplings of the h_2, h_3, a_2 could lead to an observable signal. This same question of course applies to the H and A of the MSSM. The answer there is that high $\tan\beta$ is required, in which case $gg \rightarrow b\bar{b}H, b\bar{b}A$ production is highly enhanced since the H, A have $b\bar{b}$ coupling strength of order $\tan\beta$ times the SM-like strength. We wish to explore the extent to which this also applies in the NMSSM for the h_2, h_3, a_2 in scenarios with large $\text{Br}(h_1 \rightarrow a_1 a_1)$. For this purpose, we present some additional plots in the case of $\tan\beta = 50$. We will denote the strength of the $b\bar{b}$ coupling (generally any down-type quark or lepton) of any given Higgs boson relative to the SM-like strength by $C_d(h)$, where $h = a_2, h_2, h_3$ will be considered. The relevant plots appear in Fig. 24.

In the left-hand plots of Fig. 24, we give m_{h_2} vs. m_{a_2} , m_{h_3} vs. m_{a_2} and m_{h_3} vs. m_{h_2} . The light (cyan) points are those that have both $m_{a_1} < 2m_b$ and $\text{Br}(h_1 \rightarrow a_1 a_1)$ large enough to escape the LEP limits on the $Z + 2b$ channel. For such points, the smallest allowed values of m_{a_2} , m_{h_2} and m_{h_3} are about 120 GeV, 105 GeV and 180 GeV. We see that at low $m_{a_2} < 200$ GeV, $m_{h_2} \sim m_{a_2}$, while at large $m_{a_2} > 600$ GeV one finds $m_{a_2} \sim m_{h_3}$. At intermediate m_{a_2} , one can have either degeneracy. On the right-hand side of Fig. 24, we plot the relative coupling strength C_d of each of the heavier Higgs bosons as a function of its mass. Correlating with the mass plots, we observe that for $m_{a_2} \lesssim 200$ GeV it is always the h_2 that is degenerate with the a_2 and that both have $C_d \sim \tan\beta$. For $m_{a_2} \gtrsim 600$ GeV, we always have $m_{h_3} \sim m_{a_2}$ and $C_d(h_3)$ and $C_d(a_2)$ are both $\sim \tan\beta$. For m_{a_2} in the intermediate mass range, the situation is more complicated and we can get cases where $m_{a_2} \sim m_{h_2} \sim m_{h_3}$ and

while $C_d(a_2) \sim \tan \beta$ one finds that the h_2 and h_3 can share the $\tan \beta$ enhancement factor. This is illustrated in Fig. 25.

Overall, it is clear that if $\tan \beta$ is large a search at the LHC in channels such as $gg \rightarrow b\bar{b} + Higgs$ could reveal a signal so long as m_{a_2} is not too large. For $m_{a_2} \lesssim 250$ GeV, the Tevatron might also be able to detect this kind of signal when $\tan \beta$ is large enough.

IV. CONCLUSIONS

Eliminating EWSB fine tuning in supersymmetric models has become an important issue. In the NMSSM, this is most easily achieved by allowing the lightest Higgs boson, h_1 , to have mass of order 100 GeV, as naturally predicted after radiative corrections for stop masses in the range of a few hundred GeV. The modest stop masses imply no significant fine-tuning. However, such an h_1 is typically Standard Model like in its ZZ coupling and can escape LEP limits only if the dominant decay is $h_1 \rightarrow a_1 a_1$ (so that the $h_1 \rightarrow b\bar{b}$ decay is sufficiently suppressed to escape LEP limits) and if $m_{a_1} < 2m_b$ (so that the $a_1 a_1$ final state does not feed into the $Z + b's$ final state that is strongly constrained by LEP data). In this paper, we have considered the degree to which the GUT-scale soft-SUSY-breaking parameters must be tuned in order to have $m_{a_1} < 2m_b$ and $\text{Br}(h_1 \rightarrow a_1 a_1) > 0.7$ (the rough requirement for suppressing the $h_1 \rightarrow b\bar{b}$ mode sufficiently). We have found that such a scenario need not have significant tuning. We began by assessing the tuning required of the m_Z -scale parameters $A_\lambda(m_Z)$ and $A_\kappa(m_Z)$ that primarily control both m_{a_1} and $\text{Br}(h_1 \rightarrow a_1 a_1)$. This tuning was quantified via

$$F_{MAX} \equiv \max \{|F_{A_\lambda}|, |F_{A_\kappa}|\} , \quad F_A \equiv \frac{\partial \log m_{a_1}^2}{\partial \log A} , \quad (39)$$

evaluated at scale m_Z . We found that so long as μ is not too large ($|\mu| \lesssim 200$ GeV) then the values of $A_\kappa(m_Z)$ and $A_\lambda(m_Z)$ need only be tuned to a level of order $F_{MAX} \sim 10 - 20$, corresponding to tuning in the range of 5% to 10%, for the magnitudes of $A_\kappa(m_Z)$ and $A_\lambda(m_Z)$ that are of order those automatically generated by radiative evolution from small GUT scale values. Further, these same RGE-generated values automatically give the required large values of $\text{Br}(h_1 \rightarrow a_1 a_1)$. We also discussed how these tuning estimates based on F_{MAX} will generically greatly overestimate the tuning with respect to GUT-scale soft-SUSY-breaking parameters. In any SUSY scenario in which $A_\lambda(m_Z)$ and $A_\kappa(m_Z)$ deriving

from RG evolution are dominated by a GUT-scale parameter or model-correlated set of GUT-scale parameters, generically denoted by p , the tuning with respect to p is given by $f_p \sim F_{A_\lambda} + F_{A_\kappa}$ and for the $A_\lambda(m_Z)$ and $A_\kappa(m_Z)$ regions with $m_{a_1} < 2m_b$ and $\text{Br}(h_1 \rightarrow a_1 a_1) > 0.7$ one finds $F_{A_\lambda} \sim -F_{A_\kappa}$. As a result f_p can easily be very modest in size, even for quite large μ — the opposite-sign correlation becomes increasingly effective as μ increases.

Thus, we have demonstrated that GUT-scale parameters can be chosen so that fine-tuning can essentially be eliminated for the NMSSM scenario of a light Higgs with $m_{h_1} \sim 100$ GeV, decaying primarily via $h_1 \rightarrow a_1 a_1$ with $m_{a_1} < 2m_b$ and $\text{Br}(h_1 \rightarrow a_1 a_1) \gtrsim 0.7$ (both being required to escape LEP limits). We regard this scenario (or something similar) as a highly attractive possibility for the Higgs sector. It solves both the μ problem and the fine-tuning problem. It does, however, introduce the need for proving viability of LHC discovery modes involving $h_1 \rightarrow a_1 a_1 \rightarrow 4\tau$ or 4 jets , where the jets could be c, g, s, \dots . The 4 jets mode is certain to be quite difficult to probe at the LHC — only diffractive $pp \rightarrow ppX$ might provide a signal in the form of a bump in the M_X distribution at m_{h_1} . In this regard, it is important to note that our work shows that minimizing the GUT-scale fine-tuning measure f_p appears to mildly prefer $m_{a_1} > 2m_\tau$. Thus, a strong effort should be made to develop $h_1 \rightarrow a_1 a_1 \rightarrow 4\tau$ discovery modes at the LHC and to see if LEP data can constrain this possibility. Of course, discovery of the h_1 at the ILC through a bump at $M_X = m_{h_1}$ in the $e^+e^- \rightarrow Z^* \rightarrow ZX$ channel will be extremely easy.

Acknowledgments

RD thanks K. Agashe, P. Schuster, M. Strassler and N. Toro for discussions. RD is supported by the U.S. Department of Energy, grant DE-FG02-90ER40542. Thanks go to the Galileo Galilei Institute (JFG) and the Aspen Center for Physics (JFG and RD) for hospitality and support during the course of this research. JFG also thanks M. Schmaltz for helpful conversations. JFG is supported by DOE grant #DE-FG02-91ER40674 and by the U.C. Davis HEFTI program.

-
- [1] K. Choi, K. S. Jeong and K. i. Okumura, JHEP **0509**, 039 (2005) [arXiv:hep-ph/0504037];
M. Endo, M. Yamaguchi and K. Yoshioka, Phys. Rev. D **72**, 015004 (2005)
[arXiv:hep-ph/0504036]; A. Falkowski, O. Lebedev and Y. Mambrini, JHEP **0511**, 034 (2005)
[arXiv:hep-ph/0507110]; K. Choi, K. S. Jeong, T. Kobayashi and K. i. Okumura, Phys. Lett.
B **633**, 355 (2006) [arXiv:hep-ph/0508029]; R. Kitano and Y. Nomura, Phys. Lett. B **631**, 58
(2005) [arXiv:hep-ph/0509039]; O. Lebedev, H. P. Nilles and M. Ratz, arXiv:hep-ph/0511320.
 - [2] R. Dermisek and H. D. Kim, Phys. Rev. Lett. **96**, 211803 (2006) [arXiv:hep-ph/0601036];
R. Dermisek, H. D. Kim and I. W. Kim, arXiv:hep-ph/0607169.
 - [3] R. Dermisek and J. F. Gunion, Phys. Rev. Lett. **95**, 041801 (2005) [arXiv:hep-ph/0502105];
 - [4] H. P. Nilles, M. Srednicki and D. Wyler, Phys. Lett. B **120** (1983) 346. J. M. Frere,
D. R. T. Jones and S. Raby, Nucl. Phys. B **222** (1983) 11. J. P. Derendinger and C. A. Savoy,
Nucl. Phys. B **237** (1984) 307. J. R. Ellis, J. F. Gunion, H. E. Haber, L. Roszkowski and
F. Zwirner, Phys. Rev. D **39** (1989) 844. M. Drees, Int. J. Mod. Phys. A **4** (1989) 3635.
U. Ellwanger, M. Rausch de Traubenberg and C. A. Savoy, Phys. Lett. B **315** (1993) 331
[arXiv:hep-ph/9307322], and Nucl. Phys. B **492** (1997) 21 [arXiv:hep-ph/9611251], S. F. King
and P. L. White, Phys. Rev. D **52** (1995) 4183 [arXiv:hep-ph/9505326]. F. Franke and H. Fraas,
Int. J. Mod. Phys. A **12** (1997) 479 [arXiv:hep-ph/9512366].
 - [5] U. Ellwanger, J. F. Gunion and C. Hugonie, arXiv:hep-ph/0406215.
 - [6] J. F. Gunion, H. E. Haber and T. Moroi, J.F. Gunion, H.E. Haber and T. Moroi, in the
proceedings of the DPF / DPB Summer Study on New Directions for High-Energy Physics
(Snowmass 96), Snowmass, Colorado, eConf **C960625**, LTH095 (1996), hep-ph/9610337.
 - [7] R. Dermisek and J. F. Gunion, Phys. Rev. D **73**, 111701 (2006) [arXiv:hep-ph/0510322].
 - [8] R. Dermisek and J. F. Gunion, UCD-HEP-2007-01, to appear.
 - [9] B. A. Dobrescu, G. Landsberg and K. T. Matchev, Phys. Rev. D **63**, 075003 (2001)
[arXiv:hep-ph/0005308]. B. A. Dobrescu and K. T. Matchev, JHEP **0009**, 031 (2000)
[arXiv:hep-ph/0008192].
 - [10] P. C. Schuster and N. Toro, arXiv:hep-ph/0512189.
 - [11] S. Chang, P. J. Fox and N. Weiner, arXiv:hep-ph/0511250.
 - [12] V. Barger, P. Langacker, H. S. Lee and G. Shaughnessy, Phys. Rev. D **73**, 115010 (2006)

- [arXiv:hep-ph/0603247].
- [13] M. J. Strassler and K. M. Zurek, arXiv:hep-ph/0604261.
 - [14] L. M. Carpenter, D. E. Kaplan and E. J. Rhee, arXiv:hep-ph/0607204.
 - [15] P. W. Graham, A. Pierce and J. G. Wacker, arXiv:hep-ph/0605162.
 - [16] M. J. Strassler and K. M. Zurek, arXiv:hep-ph/0605193.
 - [17] A. Arhrib, K. Cheung, T. J. Hou and K. W. Song, arXiv:hep-ph/0606114.
 - [18] M. J. Strassler, arXiv:hep-ph/0607160.
 - [19] R. Dermisek, J. F. Gunion and B. McElrath, arXiv:hep-ph/0612031.